

1 This is an accepted manuscript of an article published by Highwire in
2 Applied and Environmental Microbiology (accepted February 23 2018)
3 available at:

4 <https://doi.org/10.1128/AEM.00154-18>.

5 =====

6

7

8 **On the enigma of glutathione dependent styrene**
9 **degradation in *Gordonia rubripertincta* CWB2**

10

11 **Thomas Heine^{1,#}, Juliane Zimmerling¹, Anne Ballmann¹, Sebastian Bruno**
12 **Kleeberg¹, Christian Rückert², Tobias Busche², Anika Winkler², Jörn**
13 **Kalinowski², Ansgar Poetsch^{3,4}, Anika Scholtissek¹, Michel Oelschlägel¹, Gert**
14 **Schmidt⁵ and Dirk Tischler^{1,6,#}**

15

16 ¹Institute of Biosciences, TU Bergakademie Freiberg, Leipziger Str. 29, Freiberg,
17 Germany.

18 ²Technologieplattform Genomik, Centrum für Biotechnologie (CeBiTec), Universität
19 Bielefeld, Universitätsstr. 27, Bielefeld, Germany.

20 ³Plant Biochemistry, Ruhr University Bochum, 44801 Bochum, Germany

21 ⁴School of Biomedical and Healthcare Sciences, Plymouth University, Plymouth PL4
22 8AA, UK

23 ⁵Institut für Keramik, Glas- und Baustofftechnik, TU Bergakademie Freiberg,
24 Agricolastr. 17, Freiberg, Germany.

25 ⁶Microbial Biotechnology, Ruhr University Bochum, 44801 Bochum, Germany

26

27

28 #For correspondence. E-mail heinet@tu-freiberg.de, dirk-tischler@email.de; Tel. +49

29 3731 392103.

30

31 Running title: Styrene degradation via glutathione-S-transferase

32

33 **ABSTRACT**

34 Among bacteria, only a single styrene specific degradation pathway has been
35 reported so far. It comprises the activity of styrene monooxygenase, styrene oxide
36 isomerase and phenylacetaldehyde dehydrogenase yielding phenylacetic acid as
37 central metabolite. The alternative route comprises ring-hydroxylating enzymes and
38 yields vinyl catechol as central metabolite, which undergoes *meta*-cleavage. This was
39 reported to be unspecific and also allows the degradation of benzene derivatives.
40 However, some bacteria had been described to degrade styrene but do not employ
41 one of those routes or only parts of them. Herein we describe a novel “hybrid”
42 degradation pathway for styrene located on a plasmid of foreign origin. As putatively
43 also unspecific, it allows metabolizing chemically analogous compounds (e.g.
44 halogenated and/or alkylated styrene derivatives). *Gordonia rubripertincta* CWB2 was
45 isolated with styrene as sole source of carbon and energy. It employs an assembled
46 route of the styrene side chain degradation and isoprene degradation pathways that
47 also funnels into phenylacetic acid as central metabolite. Metabolites, enzyme
48 activity, genome, transcriptome and proteome data reinforce the observation and
49 allow to understand this biotechnologically relevant pathway which can be used for
50 the production of ibuprofen.

51 **IMPORTANCE**

52 Degradation of xenobiotics by bacteria of high interest for bioremediation, but
53 also as involved enzymes are potential catalysts in biotechnological applications.
54 This study reveals a novel degradation pathway for the hazardous organic compound
55 styrene in *Gordonia rubripertincta* CWB2. It is an impressive illustration of horizontal
56 gene transfer, which enables novel metabolic capabilities. This study presents
57 glutathione-dependent styrene metabolization in an (actino-)bacterium. Further, the

58 genomic background of the ability of strain CWB2 to produce ibuprofen is
59 demonstrated.

60

61 **INTRODUCTION**

62 Styrene is a monoaromatic compound that naturally occurs as a component of
63 tar, volatile and oily substances from plants and food, but can also be produced by
64 microorganisms. Styrene is of high relevance in industry and produced in million
65 tonne scale causing substantial anthropogenic release. This is problematic as it is
66 hazardous for living organisms (1–3). Due to the disposability, it is corollary that
67 organisms evolved strategies to detoxify and/or use styrene as a source of energy
68 and carbon (3–5).

69 Styrene can be channelled through different unspecific degradation pathways due
70 to relaxed substrate specificity of the respective enzymes (see supplemental material
71 and 3 for details). However, only one styrene specific degradation pathway is known
72 and seems to be favoured by microorganisms under aerobic conditions (3, 5, 6). This
73 upper degradation pathway is initiated by oxidation of the vinyl side chain. A styrene
74 monooxygenase (SMO) produces (S)-styrene oxide, which is converted by a
75 membrane bound styrene oxide isomerase (SOI) to phenylacetaldehyde. A
76 phenylacetaldehyde dehydrogenase (PAD) oxidizes the aldehyde to phenylacetic
77 acid (PAA) (7). PAA is a central catabolite and metabolized in the so-called lower
78 degradation pathway, which is present in about 16% of all genome-sequenced
79 microorganisms (8, 9). That route has been described for several proteobacteria
80 (*Pseudomonas*, *Xanthobacter*, *Sphingopyxis*), actinobacteria (*Rhodococcus*,
81 *Corynebacterium*) and fungi (*Exophiala*) (reviewed by 3).

82 *Rhodococcus* sp. ST-10 has an incomplete degradation cluster lacking the SOI,

83 while still being able to use styrene as sole source of carbon and energy (10–13).
84 This gene cluster comprises the SMO and a putative (partial) open reading frame
85 (ORF), designated as “ORF3”. It was hypothesized that the SOI can be bypassed by
86 chemical conversion of styrene oxide to phenylacetaldehyde or enzymatically (12–
87 14). However, chemical conversion is unlikely and no probable enzymes were
88 identified (3), thus the degradation pathway for strain ST-10 remains unclear.

89 The genus *Gordonia* is known to be a versatile degrader of aromatic compounds
90 (15, 16) and *Gordonia rubripertincta* CWB2 in particular is able to metabolize styrene
91 and related compounds. As previously described, strain CWB2 was obtained from a
92 soil sample and separated via styrene-enrichment culture (17–19). Moreover, it was
93 shown that it is able to produce ibuprofen from 4-isobutyl- α -methylstyrene in a co-
94 metabolic process (17, 18). Oelschlägel *et al.* 2015 reported that other styrene
95 degraders are not capable to catalyze this reaction and therefore proposed
96 substantial differences in the respective enzymatic cascades. Interestingly, *Gordonia*
97 *rubripertincta* CWB2 has a cluster that is homolog to the partial one of strain ST-10.

98 In this study, we identified the complete gene cluster, which enables styrene
99 degradation in strain CWB2. Therefore, we studied the transcriptome and the
100 proteome under styrene exposure. Further, we measured the activity of key enzymes
101 to clarify the root of the metabolic potential of *Gordonia rubripertincta* CWB2.
102 Moreover, this gene cluster seems to be alien as it is located on a plasmid and
103 assigned as genomic island if compared to the rest of the genome. It embodies a
104 hybrid of several homolog epoxide and aromatic compound degradation clusters from
105 different actinobacteria.

106

107 RESULTS

108 **Identification and annotation of gene clusters associated with styrene**
109 **degradation.** Genes that might be involved in styrene degradation in *G.*
110 *rubripertincta* CWB2 were identified and annotated by homology search using the
111 BLASTP algorithm (20) on the non-redundant protein database or the UniProtKB
112 database (NCBI). The annotation of the putative styrene degradation cluster with
113 respect to the closest (characterized) homolog is listed in Table 2 and Dataset S1. A
114 32424-bp cluster with 36 putative open reading frames (*orf*) was identified on the
115 plasmid pGCWB2 (~ 100 kbp), which is framed by a styrene monooxygenase
116 (*GCWB2_24100*) and phenylacetaldehyde dehydrogenase (*GCWB2_23925*).
117 Interestingly, the average GC content of this cluster is 62.11% and thus 5% lower as
118 for the whole genome. The GC content of the whole plasmid is 3% lower compared
119 to the chromosome. Besides a high amount of hypothetical proteins, pGCWB2
120 contains 4 transposase-family proteins, 2 integrase-like proteins, one relaxase-like
121 protein and one type IV secretory system as an inventory for gene mobility. Genomic
122 island analysis on the whole genome illustrates that at least parts of this styrene
123 degradation cluster have foreign origin (Fig. 1).

124 The cluster can be separated into 4 subclusters comprised as follows: cluster S1
125 contains a styrene monooxygenase, which is known to initiate the styrene
126 degradation at the vinyl side chain. The closest characterized homolog of this protein
127 was found in *Rhodococcus* sp. ST-10 (StyA – 86% identity at amino acid level; StyB
128 – 82%). A phylogenetic analysis of the amino acid sequence classifies it as an E1-
129 type SMO (Fig. S2). The closest match within *Gordonia* species is a putative
130 monooxygenase from *Gordonia polyisoprenivorans* NBRC 16320 (GAB22407 – 45%;
131 GAB22406 – 39%). However, also the genetic organisation refers to a close relation

132 to the *Rhodococcus* cluster as the partial sequence of ORF_3 from strain ST-10
133 shows 67% identity to GCWB2_24090. Transmembrane domain prediction (TMHMM)
134 of GCWB2_24090 identified 4 transmembrane helices what classifies this protein as
135 hypothetical membrane associated. Beyond that, no characterized homologs and no
136 known domains are present in the database for this ORF. It has to be mentioned that
137 no styrene oxide isomerase (*styC*) gene was found on the genome of strain CWB2.

138 The second cluster S2 embeds 7 hypothetical proteins (GCWB2_24085 -
139 GCWB2_24055). Two of them are presumably soluble and the others are annotated
140 as membrane proteins, while each has one transmembrane domain. Members of
141 these clusters appear to be rare within the database and are predominantly present
142 in rhodococci. *Rhodococcus opacus* 1CP owns a homologous cluster downstream of
143 its StyABCD cluster (WP_065493732 - WP_045063326; 56 - 68%). Further,
144 *Gordonia* sp. i37 has a homologous gene cluster in the neighbourhood of a recently
145 recorded isoprene degradation cluster (contig257: WP_079929940 -
146 WP_079929944, contig258: OPX14963 - OPX14964; 56 - 74%) (21).

147 Cluster S3 encodes for proteins that might be involved in glutathione and
148 isoprene metabolism. GCWB2_24050 and GCWB2_24045 show highest identity to a
149 glutamate-cysteine ligase GshA (P9WPK7 – 33%) and a glutathione synthetase
150 GshB (P45480 – 50%) followed by a putative coenzyme A-disulfide reductase (CoA-
151 DSR). The other genes of this cluster (GCWB2_24050 - GCWB2_24010) encode for
152 a putative MarR-like transcriptional regulator, a coenzyme A-transferase, a
153 dehydrogenase, a glutathione S-transferase, a disulfidebond oxidoreductase and an
154 aldehyde dehydrogenase. The closest characterized homolog of the latter gene
155 product is the phenylacetaldehyde dehydrogenase from *Pseudomonas fluorescens*
156 ST (O06837 – 36%). Cluster S3 can also be found in *Aeromicrobium* sp. Root495

157 wherein a styrene monooxygenase is located between the CoA-DSR and the
158 transcriptional regulator. The same is true for *Nocardioides* sp. Root240 except for a
159 13983-bp insertion right after the styrene monooxygenase gene. Interestingly, the
160 closest characterized homologs of GCWB2_24025 and GCWB2_24020 can be found
161 in *Rhodococcus* sp. AD45 (WP_045063294 – 59%; WP_045063292 – 49%) and are
162 known to be a functional part of an isoprene degradation cluster which is located on a
163 megaplasmid (300 kbp) (22). In addition, homologs of other genes from cluster S3
164 can be found on this plasmid, even in a similar arrangement of parts from this cluster.
165 However, strain AD45 does not encode for a styrene monooxygenase on its genome
166 and on the other hand strain CWB2 is lacking the isoprene monooxygenase.
167 Homologous proteins from cluster S3 were recently found in *Gordonia* sp. i37 next to
168 a homologous to cluster S2 (21). The 13983-bp insertion of *Nocardioides* sp.
169 Root240 comprises a putative mce operon, a cluster of membrane proteins whose
170 specific function is unclear.

171 The putative styrene degradation cluster is completed by a fourth gene set S4
172 (GCWB2_24005 - GCWB2_23925) that encodes for proteins which are required for
173 the lower styrene degradation pathway (phenylacetic acid catabolism). The proposed
174 pathway of strain CWB2 is displayed in Figure 3b. Besides some regulatory elements
175 and a partial gene (GCWB2_24000), this cluster is homolog to that of *Rhodococcus*
176 *opacus* 1CP and can also be found in *Gordonia soli* NBRC 108243 as well as
177 *Gordonia* sp. i37 (contig69). The AraC-like transcriptional regulator (GCWB2_24005)
178 shows homology to regulators of strain 1CP, that are located before the SMO and
179 behind the PAA degradation cluster (ANS32446 – 46%; WP_061046101 – 41%).
180 However, in contrast to strain CWB2 the upper and lower styrene degradation
181 pathways are not associated in this strain. Here the genes for the conversion of
182 styrene to phenylacetic acid are located on a plasmid pR1CP1 (NZ_CP009112),

183 whereas the subsequent metabolization is encoded on the chromosome
184 (NZ_CP009111). The second transcriptional regulator (GCWB2_23980) belongs to
185 the TetR-family. Cluster S4 is terminated by a phenylacetaldehyde dehydrogenase
186 (GCWB2_23925) that is highly similar to StyD from *Rhodococcus* sp. ST-5
187 (BAL04135 – 76%). So far, a comparable genetic environment of styrene
188 monooxygenases can only be found in *Aeromicrobium* sp. Root495 and in five strains
189 of *Nocardioides* sp. (Root79, Root190, Root240, Root614, Root682). All of them were
190 isolated from *Arabidopsis* root microbiota (23).

191 As already mentioned, the whole cluster embeds 3 HTH-type regulators, which
192 are known to respond to aromatic compounds (24). They are not similar to the
193 regulation machinery as described for pseudomonads (3).

194 Besides this, the genome of strain CWB2 was examined for other genes and
195 clusters that might enable degradation of styrene or metabolites. As no styrene oxide
196 isomerase gene (*styC*) is located on the genome of strain CWB2, it might be possible
197 that this degradation step is bypassed by a styrene oxide reductase (SOR) and a
198 phenylacetaldehyde reductase (PAR). So far, there is no enzyme characterized that
199 has SOR activity and thus no comparison with strain CWB2 on DNA level is possible.
200 However, two putative ORFs (GCWB2_12345 – 70%; GCWB2_18410 – 35%) show
201 similarity to the PAR of *Rhodococcus* sp. ST-10 (BAD51480). Interestingly, the latter
202 one is part of a cluster with 8 ORFs (GCWB2_18380 - GCWB2_18415) that is
203 homolog to one in *Gordonia* sp. TY-5 (BAD03956 - BAD03963; 87 - 96%) (25). It
204 comprises a chaperonin, a putative alcohol dehydrogenase, two hypothetical proteins
205 and a putative propane monooxygenase. The monooxygenase has also resemblance
206 with a propene monooxygenase from *Mycobacterium* sp. M156 (28 - 38%) (26) but
207 also a methane monooxygenase from *Methylococcus capsulatus* Bath (29 - 34%)

208 (27). These binuclear iron monooxygenases are able to epoxidize styrene.
209 Homologous clusters can be found in several actinobacteria (28–30), for instance in
210 *R. opacus* 1CP and *Gordonia* sp. i37 (21). The other putative PAR is not part of a
211 cluster. In addition, several cytochrome P450 monooxygenases can be found on the
212 CWB2 genome, which might also be able to perform the epoxidation of styrene.

213 **Transcriptome and proteome analysis of the styrene degrader CWB2.** The
214 transcriptome and proteome of strain CWB2 was analysed to reveal the global profile
215 of genes and proteins that are involved in styrene metabolism. Therefore, fructose-
216 grown cultures served as reference condition. The transcriptome output is
217 summarized in Table S4.

218 If assuming a threshold of ≥ 1.5 (M-value), then 2.5% of the genes of strain
219 CWB2 are overexpressed under styrene exposure and 30% of these are located on
220 the plasmid (Fig. S5). It is known, that the transcriptome as the total amount of
221 mRNA does not necessarily reflect the total amount of proteins abundance in the cell.
222 However, we were able to identify 3691 proteins in the proteome of strain CWB2. If
223 assuming a threshold of 1.5 (log₂ ratio), then 7% of the proteins were highly
224 abundant, when strain CWB2 was grown on styrene (Fig. S6). The gene cluster,
225 which is framed by the styrene monooxygenase and the phenylacetaldehyde
226 dehydrogenase, is highly upregulated on transcriptome (increased on average 7-fold)
227 as well as proteome level (increased on average 6.6-fold) (Table 2 and Dataset S1).

228 **Validation of enzymatic activity of selected members of the styrene**
229 **degradation pathway.** After analysis of the genome, transcriptome and proteome of
230 strain CWB2, we screened for enzyme activities that enable styrene degradation on
231 different pathways. For that, crude extract from styrene grown biomass was
232 prepared, proteins were separated and enriched by different chromatography

233 methods. The activities were measured directly or indirectly on a spectrophotometer
234 or by quantification of the products on the reverse phase HPLC (RP-HPLC),
235 respectively (Table S5). It was possible to detect SMO activity in the crude extract
236 and to enrich the enzyme 36-fold to an activity of 6.82 mU mg⁻¹. Due to the missing
237 SOI, it was proposed that the conversion of styrene oxide is bypassed by the activity
238 of a SOR, which produces 2-phenylethanol. This is supposed to be converted to
239 phenylacetaldehyde by a PAR. Only minor activity of a PAR with 2-phenylethanol
240 was detected in crude extract. Higher activities were determined in crude extracts,
241 when styrene oxide was applied as substrate. However, this might be due to activity
242 of a GST, while residual glutathione (GSH) is present in the crude extract of strain
243 CWB2. To further prove this assumption, crude extract was assayed for GST activity
244 after supply of additional GSH. Thereby, a GST activity of 44.23 U mg⁻¹ was reached
245 for the conversion of styrene oxide (Fig. 2).

246 Further, crude extracts were assayed for vinylcatechol-2,3-dioxygenase and
247 *cis,cis*-muconate cycloisomerase (MCI) to exclude other degradation pathways.
248 However, there was no detectable activity for one of these enzymes.

249 Two putative SMOs of strain CWB2 were cloned and expressed for initial
250 characterization. Of the two putative SMOs, only one was expressed and synthesised
251 in an active form. It is part of the styrene degradation cluster (S1; GCWB2_24100)
252 and produces (*S*)-styrene oxide with a specific activity of 0.42 ± 0.02 U mg⁻¹. The
253 SMO can be classified as E1-type SMO (Fig. S2). PADs are aldehyde
254 dehydrogenases that catalyze the formation of the central intermediate phenylacetic
255 acid. Two aldehyde dehydrogenases of strain CWB2 were recombinantly expressed
256 in *E. coli*. Aldh1 which originates from the isoprene degradation cluster (S3) catalyzes
257 the conversion of phenylacetaldehyde with an activity of 0.29 ± 0.01 U mg⁻¹. StyD,

258 which is encoded in cluster S4 is 10-times slower and has an activity of 0.026 ± 0.001
259 U mg⁻¹.

260

261 **DISCUSSION**

262 **Adaption of *G. rubripertincta* CWB2 to styrene exposure.** Only few reports
263 exist for *Gordonia* considering the metabolization of styrene (18, 31). Further, the
264 limited amount of SMOs that are encoded on genomes of this genus indicate that
265 styrene degradation is no common feature. *Gordonia rubripertincta* CWB2 is able to
266 withstand and degrade high amounts of styrene (520 g m⁻³ in 21 h), even compared
267 to other efficient styrene degraders (32, 33). Some bacteria produce surfactants,
268 when they are exposed to hydrophobic substrates, to increase their accessibility (34–
269 36). However, we found no indication that strain CWB2 exports biosurfactants into
270 the media but it seems to have a hydrophobic cell surface, which improves substrate
271 uptake. This is supported by a tendency to form agglomerates during growth in liquid
272 media.

273 There is no complete prokaryotic transcriptome under styrene exposure available
274 yet. So far, studies focused on the transcriptional regulation of styrene degradation
275 and a small number of target genes, solely with respect to *Pseudomonas* strains (37–
276 44). A proteome of *R. jostii* RHA1, which employs an unspecific styrene degradation
277 route, is available (45). So far, only one system level proteome analysis for styrene
278 degradation in *P. putida* CA-3 exists (46). It was the first time where all of the
279 respective enzymes of the upper and lower degradation pathway were detected,
280 when a strain was grown on styrene (46).

281 Omic analysis of strain CWB2 in this study outlines the biological background for
282 its adaption to styrene as source of carbon and energy. This was found to be totally

283 different to so far characterized styrene degraders. Initially styrene has to be
284 imported into the cell. The only specific styrene transporter StyE was found in
285 pseudomonads (47). However, the *styE* gene is not encoded in most other styrene
286 degraders and thus, other transport mechanisms as well as diffusion have to be
287 considered (3, 46). Cluster S2 of strain CWB2 contains several membrane proteins
288 that are highly upregulated and the same cluster is also present in the styrene
289 degrader *R. opacus* 1CP (Fig. 1). Thus, it is likely that these proteins might also be
290 involved in substrate transport or cell membrane adaption. Interestingly, *Gordonia* sp.
291 i37 owns a similar cluster in proximity of an isoprene degradation cluster (21).
292 However, there are no characterized homologs available in the database and thus
293 the specific function of these proteins remains unclear.

294 **Strain CWB2 merged clusters to form a hybrid that enables styrene**
295 **degradation.** The genetic organisation of the putative styrene degradation cluster
296 compared to other clusters with homolog proteins can be found in Figure 1. The
297 “classical” styrene degradation cluster of *Pseudomonas* sp. Y2 differs to
298 *Rhodococcus* clusters as well as the recently reported cluster of *S. fribergensis* Kp5.2
299 (17, 38, 48). Thus, it is obvious that the arrangement and regulation is variable
300 among different organisms. The styrene degradation cluster of strain CWB2 is highly
301 upregulated on mRNA and protein level, when strain CWB2 grows on styrene (Table
302 2 and Dataset S1). In *Pseudomonas putida* CA-3 the SMO and PAD were the most
303 abundant proteins (46). In strain CWB2 they are also highly upregulated but in a
304 comparable range to the rest of the genes and proteins of this cluster. It can be seen
305 that the transcriptional regulators (GCWB2_24035; GCWB2_23980) are less
306 expressed and synthesized. It is also obvious that regulation of gene expression
307 differs in strain CWB2 as no StyR/StyS homolog is associated to this cluster.

308 However, further studies with different inducers are necessary to clarify the
309 regulation.

310 There is no evidence that strain CWB2 performs direct ring cleavage of styrene or
311 activation by an epoxide hydrolase as the respective parts of these pathways are not
312 present on the genome or upregulated in the transcriptome or proteome, when
313 cultivated on styrene (supplemental material). In contrast, initial epoxidation of
314 styrene was found to be catalyzed by a SMO. Enzyme activity was detected in crude
315 extracts of styrene-grown cells and the SMO was successfully enriched by ion-
316 exchange chromatography and hydrophobic interaction chromatography (Table S5).
317 The SMO (GCWB2_24100; ASR05591) was recombinantly expressed and purified.
318 The specific epoxidation activity is about 0.4 U mg⁻¹ and thus higher than for most
319 other characterized SMOs (48–50). However, epoxidation of styrene is usually the
320 rate-limiting step due to the relative low activity of the SMOs (51).

321 The SMO is part of cluster S1, which is highly similar to the partial styrene
322 degradation cluster of *Rhodococcus* sp. ST-10. Toda and co-workers proposed
323 chemical conversion of styrene oxide or the cooperation of a styrene oxide reductase
324 (SOR) and phenylacetaldehyde reductase (PAR) (12, 13) as no SOI is present in this
325 strain. However, previous as well as this study indicate that this is rather unlikely, as
326 we detected only minor SOR and PAR activity in the crude extract of strain CWB2.
327 Both assumptions would not explain fast degradation of styrene as found in these
328 strains (3, 52, 53). However, strain ST-10 accumulated the epoxide when incubated
329 with styrene and thus it remains to be shown if the rest of the genes are also
330 homolog to the styrene degradation cluster in strain CWB2.

331 To circumvent this missing link of enzymatic styrene oxide isomerization, strain
332 CWB2 seems to have incorporated a cluster (S3), which is very similar to ones from

333 *Aeromicrobium* sp. Root495 and *Nocarioiodes* sp. Root240. Interestingly, both were
334 isolated at the same site (23) and both clusters are as well closely located to a
335 styrene monooxygenase in these strains. The genes of cluster S3 may originate from
336 an isoprene degradation cluster as found on a megaplasmid in *Rhodococcus* sp.
337 AD45 (AJ249207) but also in *Gordonia* sp. i37 (21, 54). Actinobacteria from the
338 genera *Mycobacterium*, *Rhodococcus* and *Gordonia* were constantly detected in
339 different environments as isoprene degraders (21, 54, 55). *Rhodococcus* sp. AD45
340 initially epoxidizes isoprene by the activity of an isoprene monooxygenase. Then it
341 uses a glutathione S-transferase to convert the epoxide to a glutathione-alcohol
342 adduct, which is further metabolized by a dehydrogenase to form an aldehyde and
343 subsequently an acid (22, 54, 56–59). Remarkably, strain AD45 is also able to
344 metabolize styrene but has no SMO (56). Derived from these observations, it might
345 be possible that styrene is also channelled through the isoprene degradation
346 pathway in *G. rubripertincta* CWB2. Further, strain CWB2 owns genes that are
347 necessary for glutathione synthesis and reduction in cluster S3 (60). Interestingly,
348 strain CWB2 does not possess an isoprene monooxygenase and has no ability to
349 catabolize isoprene (Table 1).

350 **Styrene oxide is channelled into a novel glutathione dependent degradation**
351 **pathway.** To proof, whether glutathione dependent metabolization occurs, we
352 assayed crude extract from styrene grown cells for GST activity with (S)-styrene
353 oxide as substrate. We found that the epoxide was degraded fast with an activity of
354 44 U mg_{crude extract}⁻¹ (Fig. 2). Only minor activity was detected when no reduced
355 glutathione was added to the reaction.

356 Therefore, we propose a novel degradation pathway for styrene via initial
357 epoxidation by a SMO to (S)-styrene oxide and addition of glutathione by the GST

358 Styl (Fig. 3a). The resulting (S)-(1-Phenyl-2-hydroxyethyl) glutathione (CAS: 64186-
359 97-6) will be further converted by the dehydrogenase StyH to (S)-(1-Phenyl-2-
360 acetaldehyde) glutathione and (S)-(1-Phenyl-2-acetic acid) glutathione. It might be
361 possible that the phenylacetaldehyde dehydrogenase (PAD) and/or the aldehyde
362 dehydrogenase (Adh1) are also involved in this step as both showed activity with
363 phenylacetaldehyde (61). As the glutathione adduct is not easily accessible it has to
364 be verified if the Adh1 and the PAD can also catalyze this reaction. It was shown that
365 the aldehyde dehydrogenase of cluster S3 are induced in strain AD45 but no specific
366 role had been ascribed (22). Subsequently the glutathione is removed from the
367 adduct what might occur by the activity of StyJ and StyG (58, 62, 63). The product of
368 this process will be phenylacetic acid or phenylacetyl-CoA, which will be degraded
369 via several enzymes from cluster S4 to yield acetyl-CoA and succinyl-CoA (Fig. 3b).
370 We suppose that the 2-phenylethanol and phenylacetaldehyde, that can be detected
371 during growth, results from side-product formation of this novel pathway due to
372 instability of the glutathione adducts or enzymatic removal of glutathione in an earlier
373 step (Fig. 3a).

374 It should be mentioned that it is unusual for actinobacteria to produce glutathione,
375 as mycothiol is the dominant thiol in these organisms (64–66). However, it was
376 reported that strain AD45 additionally produces substantial amounts of glutathione
377 and it was suggested that this ability was gained by horizontal gene transfer of
378 isoprene degradation genes (54, 56, 58, 65). It is likely that the same is true for strain
379 CWB2 due to the plasmid uptake. This is supported by the finding that the GC
380 content of the plasmid and the styrene degradation cluster is much lower compared
381 to the whole genome. The GC content of that cluster S3 is close to that of strain
382 AD45 (61.7%; (22). Recently, genes of cluster S3 were found in *Gordonia* sp. i37
383 (21). Further, strain CWB2 as well as strain 1CP encode for several mobile elements

384 in direct neighbourhood of the styrene degradation cluster on their plasmid what
385 suggests horizontal gene transfer. In addition, the cluster S4 is highly similar that that
386 of *R. opacus* 1CP and strain RHA1 and degradation of PAA likely takes place in the
387 same way (67, 68) (Fig. 3b).

388

389 **CONCLUSION**

390 Omic analyses imply that strain CWB2 incorporated a plasmid which contains an
391 assembly of different gene clusters and forms a “hybrid” that enables to metabolize
392 styrene and analogous compounds. Our study illustrates the possibilities of horizontal
393 gene transfer for Gram-positive bacteria and an ongoing adaptation to glutathione as
394 cofactor in actinobacteria. This adaption is coupled with a high biotechnological
395 potential of this organism, as *G. rubripertincta* CWB2 can produce ibuprofen, which is
396 not possible through the classical styrene degradation pathway (17, 18). The
397 involved SMO shows higher activities than reported for other SMOs so far. This might
398 be interesting as these enzymes are known to catalyze a variety of valuable reactions
399 (3). Further, bacterial GST are known to be involved in degradation of (halogenated)
400 xenobiotics and other chemical transformations and therefore the GST of strain
401 CWB2 might open a new field of possible biochemical reactions to this class of
402 enzymes (63, 69, 70).

403 MATERIALS AND METHODS

404 **Isolation and cultivation of styrene-degrading strains.** Styrene degrading
405 bacteria were isolated from (contaminated) soil. A small amount of the soil was
406 transferred into a 1-l Erlenmeyer flask and suspended in 100 ml water. Portions of 10
407 to 40 μ l of styrene were supplied via an evaporation adaptor as sole source of carbon
408 and energy. The growth media was dosed with 0.02 mg ml⁻¹ nalidixic acid and 0.075
409 mg ml⁻¹ cycloheximide to prevent growth of Gram-negative bacteria or fungi,
410 respectively. 10 ml of the culture was plated on solid mineral medium (MM) (71)
411 without carbon source and incubated at room temperature in a 5-l desiccator under
412 styrene containing atmosphere. The grown colonies were repeatedly transferred on
413 fresh solid mineral media and incubated for 2 - 3 days in the desiccator. The isolates
414 were stored at - 80°C in 40% (v/v) glycerol.

415 Liquid cultures were kept in Erlenmeyer flasks containing mineral media (71). The
416 respective carbon source was added either directly into the media or in case of
417 volatile compounds via an evaporation adapter.

418 **Characterization of *G. rubripertincta* CWB2.** Growth of strain CWB2 in liquid
419 MM was assayed on various substrates (Table S1). Production of surfactants with
420 fructose, hexadecane or styrene as carbon source was examined as published
421 earlier (36, 72). Siderophore production was determined by the CAS-agar plate test
422 (73). Analysis of the mycol- and fatty acid composition was done by the Deutsche
423 Sammlung für Mikroorganismen und Zellkulturen (DSMZ) (Table S2). 16S rRNA
424 analysis and Scanning electron microscopy (SEM) was done as described earlier
425 (18) (Fig. S1 and S3). The *in silico* DNA-DNA-hybridization was performed by the
426 Genome-to-Genome Distance Calculator 2.1 (DSMZ) (Fig. S7). *G. rubripertincta*

427 CWB2 was assayed for antibiotic resistance on chloramphenicol, ampicillin,
428 tetracycline, nalidixic acid, gentamycin, streptomycin and kanamycin.

429 **DNA extraction and genome sequencing, annotation and bioinformatic**
430 **analysis.** A 50-ml culture of *G. rubripertincta* CWB2 was grown on fructose in
431 mineral media. Cells were harvested at an OD₆₀₀ of 0.6 by centrifugation (5 000 x g;
432 15 min), washed once with 100 mM phosphate buffer (pH 7.5) and centrifuged again.
433 The cell Pellet was resuspended in 2.7 ml buffer (10 Tris-HCl, 10% sucrose, 30 mg
434 lysozyme; pH 7.8) and incubated for 1.5 h at 37°C. After centrifugation the
435 supernatant was discarded and the pellet was resuspended in 2.8 ml TE-buffer 10.1
436 (10 mM Tris, 1 mM EDTA; pH 8) with 100 µg ml⁻¹ proteinase K and 150 µl
437 SDS (10%) and incubated for 2 h at 37°C. Chromosomal DNA was extracted
438 successively with 3 to 5 ml phenol (equilibrated; 2 times), phenol:chloroform:isoamyl
439 alcohol (25:24:1) and chloroform:isoamyl alcohol (24:1; 2 times). Each extraction was
440 followed by a centrifugation (20 000 x g; 10 min) and separation of the aqueous
441 phase into a new tube. Afterwards, RNA was digested by adding 100 µg ml⁻¹ RNase
442 A at 37°C for 10 min. The DNA was precipitated on ice by the addition of 1/10 volume
443 of 3 M sodium acetate (pH 5.2) and 3 volumes of 100% ethanol. The precipitate was
444 centrifuged at 4°C, resuspended in 70% ice-cold ethanol and centrifuged again. The
445 supernatant was discarded and the pellet was dried for 10 min in a SpeedVac
446 vacuum concentrator. The pellet was dissolved in TE-buffer 10.1 for storage at 4°C
447 and purity was controlled by agarose-gel electrophoresis and on the Nanodrop.

448 To obtain the complete genome sequence, two sequencing libraries were
449 prepared, a TruSeq PCR-free whole genome shotgun library and a 8k Nextera
450 MatePair library (Illumina Inc, Netherlands). Both libraries were sequenced on an
451 Illumina MiSeq desktop sequencer with 2x 300 bp. The obtained reads were

452 assembled using the Newbler (v2.8) *de novo* assembler (Roche). The initial
453 assembly consisted of just one scaffold of 90 contigs, with 120 contigs larger than
454 500 bp in total. Manual inspection and assembly was performed using CONSED (74,
455 75), which revealed a misassembly: 3 contigs representing a 105 kbp plasmid,
456 henceforth called pGCWB2, were wrongly "attached" to the scaffold representing the
457 chromosome. The sequence of both replicons could be completely established. The
458 sequences for both replicons were annotated using PROKKA (76), see Table S3 for
459 details. The annotated replicons were submitted to GenBank, the accession numbers
460 are CP022580 (chromosome) and CP022581 (pGCWB2)

461 Additional functional annotation of proteins was done by using the BLASTP
462 algorithm (20) on the non-redundant protein database or the UniProtKB database
463 (NCBI) (date of search: 01.09.2017). Membrane association of proteins was verified
464 by prediction on the TMHMM server (77). Island viewer 4 (78) was applied to detect
465 genomic islands and foreign genes on the genome of strain CWB2 (Fig. S4).

466 **RNA extraction and transcriptome sequencing.** A pre-culture of *G.*
467 *rubripertincta* CWB2 was grown at 30°C in minimal media with fructose or styrene as
468 sole source of carbon, respectively. After 5 days of cultivation the culture was diluted
469 1/10 in fresh media and incubated for 24 h with the respective substrate in a set of
470 four Erlenmeyer flasks. Prior harvesting the cells, 10% of an ice-cold STOP-solution
471 (10% buffered phenol in ethanol) was added to the culture followed by centrifugation
472 at 11 000 x g for 5 min at 4°C. The supernatant was discarded and the pellet was
473 stored until RNA isolation at - 80°C. To break up the cells, 150 µl of a 5 mg ml⁻¹
474 lysozyme solution were added to the pellet, mixed and incubated at room
475 temperature for 5 min. 450 µl of buffer RLT (Qiagen) and 50 mg of (0.1 mm) glass
476 beads were added to resuspend and break the cells by repeated vortexing at 4°C.

477 The suspension was applied to QIAshredder column for homogenization and to
478 remove particles from the sample. Extraction of total RNA Extraction was done by
479 applying the RNeasy Mini Kit including on-column DNA digestion (Qiagen). Isolated
480 RNA was stored at - 80°C and quality was controlled on the 2100 Bioanalyzer using
481 the RNA 6000 Nano Kit (Agilent).

482 RNA quality and quantity was again checked by an Agilent 2100 Bioanalyzer run
483 (Agilent Technologies, Böblingen, Germany) and Trinean Xpose sytem (Gentbrugge,
484 Belgium) prior and after rRNA depletion by Ribo-Zero rRNA Removal Kit (Bacteria)
485 (Illumina, San Diego, CA, USA). TruSeq Stranded mRNA Library Prep Kit from
486 Illumina, (San Diego, CA, USA) was used to prepare the cDNA libraries to analyze
487 the whole transcriptome. The resulting cDNAs were then sequenced paired end on
488 an Illumina MiSeq and HiSeq 1500 system (San Diego, CA, USA) using 2 x 75 nt
489 read length. The raw sequencing read files are available in the ArrayExpress
490 database (www.ebi.ac.uk/arrayexpress) under accession number: E-MTAB-6012.
491 Reads were mapped on the reference *G. rubripertincta* CWB2 (CP022580,
492 CP022581) with Bowtie2 (79) using standard settings. ReadXplorer 2.2.0 (80) was
493 used for visualization of short read alignments and data analysis. Differential gene
494 expression analysis was performed based on normalized read count using TPM
495 values (Transcripts Per Million) of CDS calculated by ReadXplorer 2.2.0. The signal
496 intensity value (a-value) was calculated by $0.5 * (\log_2 \text{TPM condition A} + \log_2 \text{TPM}$
497 $\text{condition B})$ of each CDS and the signal intensity ratio (m-value) by the difference of
498 $(\log_2 \text{TPM})$. CDS with m-values of higher/equal than +1.5 or lower/equal than -1.5
499 were considered to be differentially transcribed.

500 **Preparation of protein samples and identification by LC-ESI-MS/MS mass**
501 **spectrometry.** *G. rubripertincta* CWB2 was grown the same way as for RNA

502 extraction in a set of four samples per carbon source. After cultivation, two samples
503 were pooled and centrifuged at 5 000 x g for 30 min at 4°C and resuspended in 2.5
504 ml 50 mM PP, pH 7.26. The cells were disrupted by sonication on ice (10 cycles, 1.5
505 min; power: 70%; BANDELIN Sonoplus Homogenisator HD2070) after adding 40 U
506 DNaseI and 1 mg ml⁻¹ lysozyme. The suspension was centrifugated at 50 000 x g for
507 1 h at 4°C to separate soluble from insoluble matter. The proteins were separated by
508 size using discontinuous sodium dodecyl sulfate-polyacrylamide gel electrophoresis
509 (SDS-PAGE) with 50 µg of each sample per lane. Lanes were cut into 8 slices and
510 de-stained, alkylated and digested with trypsin as previously described (81, 82).
511 Peptides were extracted from the gel pieces with acetonitrile, loaded onto STAGE
512 tips for storage, and eluted from the tips shortly before MS analysis (83).

513 By using an EASY- nLC 1000 (Thermo Scientific) LC system, peptides were
514 separated at a flow rate of 400 nl/min on a 18 cm self-packed column (75 µm ID, 1.9
515 µm Reprosil-Pur 120 C-18AQ beads, Dr Maisch Germany) housed in a custom-built
516 column oven (84) at 45°C. Peptides were separated using gradient of buffers A
517 (0.1% formic acid) and B (80% acetonitrile, 0.1% formic acid) from 1% to 60% B. The
518 column was interfaced with a Nanospray Flex Ion Source (Thermo Scientific) to a Q-
519 Exactive HF mass spectrometer (Thermo Scientific). MS instrument settings were:
520 1.5 kV spray voltage, Full MS at 60K resolution, AGC target 3e6, range of 300 - 1750
521 m/z, max injection time 20 ms; Top 15 MS/MS at 15K resolution, AGC target 1e5,
522 max injection time 25 ms, isolation width 2.2 m/z, charge exclusion +1 and
523 unassigned, peptide match preferred, exclude isotope on, dynamic exclusion for 20s.

524 Mass spectra were recorded with Xcalibur software 3.1.66.10 (Thermo Scientific).
525 Using a custom database containing 4831 predicted protein sequences, proteins
526 were identified with Andromeda and quantified with the LFQ algorithm embedded in

527 MaxQuant version 1.5.3.17 (85). The following parameters were used: main search
528 max. peptide mass error of 4.5 ppm, tryptic peptides of min. 6 amino acid length with
529 max. two missed cleavages, variable oxidation of methionine, protein N-terminal
530 acetylation, fixed cysteine carbamidomethylation, LFQ min. ratio count of 2, matching
531 between runs enabled, PSM and (Razor) protein FDR of 0.01, advanced ratio
532 estimation and second peptides enabled. Proteins with a log₂ ratio of higher/equal
533 than +1.5 or lower/equal than -1.5 were considered to be differentially synthesized.

534 **Cloning, expression and purification of recombinant styAs, styD and aldH1.**

535 The *styA* (GCWB2_24100, GCWB2_21620), *styD* (GCWB2_23925) and *aldH1*
536 (GCWB2_24010) genes were purchased from Eurofins MWG (Ebersberg) in a pEX-
537 K2 vector system allowing for kanamycin resistance selection. The DNA sequences
538 were optimized for the codon usage and GC content of *Acinetobacter baylyi* ADP1
539 with the OPTIMIZER tool (48, 86). 5'-NdeI and 3'-NotI restriction sites were added
540 and used for subcloning into pET16bP to obtain the expression constructs
541 pSGrA1_P01, pSGrA2_P01 and pSGrD1_P01, pSGrD2_P01 from which
542 recombinant proteins can be obtained as His₁₀-tagged proteins. *Escherichia coli*
543 strain DH5 α and strain BL21 (DE3) pLysS were cultivated for cloning and expression
544 purposes as described elsewhere (87). Plasmids are listed in Table 3.

545 Expression of StyA's took place in a 3-l biofermenter. *E. coli* BL21 strains with the
546 respective plasmids were cultivated in LB media (100 μ g ml⁻¹ ampicillin and 50 μ g ml⁻¹
547 chloramphenicol) at 30°C until an OD₆₀₀ of 0.4 was reached. The batch was
548 subsequently cooled to 20°C. Expression was induced at an OD₆₀₀ of 0.6 by adding
549 0.1 mM of IPTG (isopropyl- β -D-thiogalactopyranoside) to the culture and grown for 20
550 h at 20°C (120 rpm). Cells were harvested by centrifugation (5 000 x g, 30 min, 4°C),
551 resuspended in 10 mM Tris-HCl buffer (pH 7.5) and stored at - 80°C. Formation of

552 the blue dye indigo is observable if active SMOs are produced during expression in
553 LB media (88). As this was not the case for expression of *GCWB2_21620* we
554 assumed that the protein is not synthesized or active.

555 For purification of StyA, crude extracts were prepared from freshly thawed
556 biomass by disruption in a precooled French Pressure cell, followed by centrifugation
557 to remove cell debris (50 000 x g, 2 h, 4°C). The supernatants were applied to a 1-ml
558 HisTrap FF column. The column was washed with 10 CV of binding buffer (10 mM
559 Tris-HCl, 0.5 M NaCl, 25 mM imidazole, pH 7.5) to remove nonspecific bound
560 proteins. Enzymes were eluted with a linear imidazole gradient up to 500 mM over 30
561 CV. Fractions with respective enzyme activity (see 2.6.) were pooled and
562 concentrated using Sartorius Vivaspin 20 filters (5 000 MWCO) at 4°C. The
563 concentrates were passed through a 10-ml Econo-Pac 10DG desalting gravity-flow
564 column (Bio-Rad) to remove remaining imidazole and sodium chloride. Protein
565 obtained was kept in storage buffer (10 mM Tris-HCl, 50% [v/v] glycerol, pH 7.5) at -
566 20°C. Expression of *GCWB2_21620* did not yield active protein as already
567 mentioned. Preparation of StyD and Aldh1 was done according to Zimmerling *et al.*
568 2017 (61).

569 **Purification of wild-type proteins.** All following purification steps were
570 performed on an ÄKTA fast-performance liquid chromatographer (GE Healthcare).
571 Selected wild-type enzymes were enriched from crude extract by ion-exchange
572 chromatography. Therefore, strain CWB2 was cultivated on styrene and soluble
573 crude extract was prepared as described above. The supernatant was loaded with
574 buffer A (20 mM Tris-HCl; pH 7.5) on a MonoQ HR 5/5 column (GE Healthcare) at a
575 flow rate of 1 ml min⁻¹. Nonspecific bound proteins were removed by washing with 5
576 column volumes (CV) of buffer A. Elution of proteins was done over 25 CV with a

577 linear gradient of buffer B (20 mM Tris-HCl, 1 M NaCl; pH 7.5). Fractions of 1 ml were
578 collected and tested on the respective enzyme activity. A second purification step
579 was applied for some enzymes by using hydrophobic interaction chromatography.
580 Therefore, the fractions that showed the respective enzyme activity were pooled and
581 $(\text{NH}_4)_2\text{SO}_4$ was added to a final concentration of 460 mM. The sample was loaded
582 with buffer C (20 mM Tris-HCl, 0.8 M $(\text{NH}_4)_2\text{SO}_4$; pH 7.5) on a 1-ml Phenyl HP HiTrap
583 column (GE Healthcare) at a flow rate of 1 ml min⁻¹. Nonspecific bound proteins were
584 removed by washing with 5 column volumes (CV) of buffer A. Elution of proteins was
585 done over 25 CV with a linear gradient of buffer A (20 mM Tris-HCl; pH 7.5).
586 Fractions of 1 ml were tested on enzyme activity.

587 For VC12DO gel filtration was done after hydrophobic interaction
588 chromatography. Therefore, the fraction containing VC12DO activity were pooled and
589 applied with buffer D (25 mM Tris-HCl, 0.5 M NaCl; pH 7.5) to a Superdex 200 HR
590 10/30 column at a flow rate of 0.4 ml min⁻¹. Fractions of 1 ml were tested for VC12DO
591 activity.

592 Recombinant and wild-type proteins were subjected to discontinuous sodium dodecyl
593 sulfate-polyacrylamide gel electrophoresis (SDS-PAGE) (87) in order to determine
594 purity and subunit molecular size.

595 **Enzyme assays.** Crude extracts, enriched or purified protein preparations from
596 *G. rubripertincta* CWB2 were assayed for enzyme activities that are representative
597 for known degradation pathways of styrene.

598 Wild-type catechol 1,2-dioxygenase, catechol 2,3-dioxygenase and *cis,cis*-
599 muconate cycloisomerase activity was measured spectrophotometrically (Cary 50,
600 Varian) by following the product formation or substrate depletion according to
601 Warhurst *et al.* 1994 (89) using catechol, protocatechuate and *cis,cis*-muconate as

602 substrates, respectively.

603 Styrene monooxygenase (SMO) activity of wild-type and recombinant enzyme
604 preparations with styrene were measured by quantification of the reaction product
605 styrene oxide on a RP-HPLC system as described previously (90).

606 Styrene oxide reductase (SOR) and phenylacetaldehyde reductase (PAR) wild-
607 type activity with styrene oxide and 2-phenylethanol was determined by quantification
608 of the reaction products phenylacetaldehyde or 2-phenylethanol on a RP-HPLC
609 system following the protocol as described previously for the styrene oxide isomerase
610 (SOI) (17, 18).

611 Wild-type phenylacetaldehyde dehydrogenase (PAD) and wild-type PAR activity
612 was assayed indirectly on a spectrophotometer (Cary 50, Varian) by following the
613 reduction of NAD⁺ to NADH at 340 nm ($\epsilon_{340 \text{ nm}} = 6.22 \text{ mM}^{-1} \text{ cm}^{-1}$) (91). The 1 ml
614 assay mixture contained 0.5 mM phenylacetaldehyde or 2-phenylethanol in 10 mM
615 Tris-HCl (pH 7.5), 1 mM NAD⁺ and 50 μl protein containing sample, respectively.
616 Recombinant PAD activity was assayed according to (61).

617 GST wild-type activity was assayed in soluble crude extract by following the (S)-
618 styrene oxide consumption over time. Therefore, *G. rubripertincta* CWB2 was grown
619 on MM with styrene as sole source of carbon. A 100 ml pre-culture was prepared and
620 used to inoculate the main culture 1:50 in 500 ml fresh MM. The main culture was
621 incubated at 30°C for 5 days by adding 20 to 80 μl portions styrene via gas-phase.
622 Cells were harvested by centrifugation at 5 000 x g for 20 min at 4°C. The
623 supernatant was discarded and the pellet was resuspended and washed 2 times in
624 10 ml 20 mM PP (pH 8). The cells were disrupted by sonication on ice (10 cycles,
625 1 min; power: 70%; BANDELIN Sonoplus Homogenisator HD2070) after adding 40 U
626 DNaseI and 1 mg ml⁻¹ lysozyme. Soluble crude extracts were obtained by

627 centrifugation at 50 000 x g at 4°C for 1 h and separation from the insoluble matter.
628 The reaction mix (600 µl) contained 20 mM PP (pH 8), 4 mM (S)-styrene oxide, 5 mM
629 GSH and an appropriate amount of soluble crude extract. Blank measurements were
630 carried out by omitting either GSH or enzyme preparation. Samples were tempered
631 for 10 min at 30°C and the reaction was initiated by the addition of the substrate (S)-
632 styrene oxide. 25 µl samples were quenched at certain time points in 50 µl ice cold
633 acetonitrile:methanol (1:1) and centrifuged at 16 000 x g for 10 min at 4°C to remove
634 precipitates. Supernatants were applied to RP-HPLC by injection of 10 µl samples.
635 All measurements were done in triplicates. Enzyme activities are given in 1 U mg⁻¹
636 representing the conversion µmol substrate per min per mg protein.

637 All RP-HPLC measurements were done with a Eurospher C₁₈ column (125 mm
638 length by 4 mm i.d., 5 µm particle size, 100 Å pore size; Knauer, Germany). The
639 protein content was determined by means of the Bradford method (92), using
640 BradfordUltra reagent (Expedeon) and bovine serum albumin (Sigma) as reference
641 protein.

642 **Accession numbers.** Genome and assembly of *Gordonia rubripertincta* CWB2 is
643 deposited at NCBI (BioProject Accession: PRJNA394617; URL:
644 <https://www.ncbi.nlm.nih.gov/bioproject/?term=PRJNA394617>) with the chromosome
645 (CP022580) and plasmid (CP022581) sequences.

646 The raw sequencing read files are available in the ArrayExpress database
647 (www.ebi.ac.uk/arrayexpress) under accession number: E-MTAB-6012.

648 Newly characterized recombinant proteins in this study are StyA (ASR05591;
649 <https://www.ncbi.nlm.nih.gov/protein/ASR05591>), StyD (ASR05556;
650 <https://www.ncbi.nlm.nih.gov/protein/ASR05556>), Aldh1 (ASR05573;

651 <https://www.ncbi.nlm.nih.gov/protein/ASR05573>) and the monooxygenase
652 (ASR05096; <https://www.ncbi.nlm.nih.gov/protein/ASR05096>).

653

654 **ACKNOWLEDGEMENTS**

655 We appreciate the funding of this project by the Deutsche Bundesstiftung Umwelt
656 (DBU), the European Social Fund and the Saxonian Government (GETGEOWEB:
657 100101363).

658 We hereby declare no conflicting interests among all of us the co-authors.

659

660

661 **SUPPLEMENTAL MATERIAL**

662 Supplemental material is available at AEM's website.

663

664

665 **REFERENCES**

- 666 1. Bond JA. 1989. Review of the toxicology of styrene. *Crit Rev Toxicol* 19:227–
667 249.
- 668 2. Gibbs BF, Mulligan CN. 1997. Styrene toxicity: an ecotoxicological assessment.
669 *Ecotoxicol Environ Saf* 38:181–194.
- 670 3. Tischler D. 2015. *Microbial styrene degradation*. Springer Verlag.
- 671 4. van Agteren MH, Keuning S, Janssen DB, Janssen JP, Oosterhaven J. 2010.
672 *Handbook on biodegradation and biological treatment of hazardous organic*
673 *compounds. Environment and Chemistry, v. 2*. Springer Netherlands, Dordrecht.
- 674 5. Tischler D, Kaschabek SR. 2012. Microbial styrene degradation. From basics to
675 biotechnology, 67–99. *In* Singh SN (ed), *Microbial degradation of xenobiotics*.
676 Springer-Verlag, Berlin Heidelberg.
- 677 6. Mooney A, Ward PG, O'Connor KE. 2006. Microbial degradation of styrene:
678 biochemistry, molecular genetics, and perspectives for biotechnological
679 applications. *Appl Microbiol Biotechnol* 72:1–10.
- 680 7. Crabo AG, Singh B, Nguyen T, Emami S, Gassner GT, Sazinsky MH. 2017.
681 Structure and biochemistry of phenylacetaldehyde dehydrogenase from the
682 *Pseudomonas putida* S12 styrene catabolic pathway. *Arch Biochem Biophys*
683 616:47–58.
- 684 8. Teufel R, Mascaraque V, Ismail W, Voss M, Perera J, Eisenreich W, Haehnel W,
685 Fuchs G. 2010. Bacterial phenylalanine and phenylacetate catabolic pathway
686 revealed. *Proc Natl Acad Sci USA* 107:14390–14395.
- 687 9. Grishin AM, Cygler M. 2015. Structural organization of enzymes of the
688 phenylacetate catabolic hybrid pathway. *Biology (Basel)* 4:424–442.
- 689 10. Itoh N, Yoshida K, Okada K. 1996. Isolation and identification of styrene-
690 degrading *Corynebacterium* strains, and their styrene metabolism. *Biosci*
691 *Biotechnol Biochem* 60:1826–1830.
- 692 11. Itoh N, Hayashi K, Okada K, Ito T, Mizuguchi N. 1997. Characterization of
693 styrene oxide isomerase, a key enzyme of styrene and styrene oxide metabolism
694 in *Corynebacterium* sp.. *Biosci Biotechnol Biochem* 61:2058–2062.
- 695 12. Itoh N, Morihama R, Wang J, Okada K, Mizuguchi N. 1997. Purification and
696 characterization of phenylacetaldehyde reductase from a styrene-assimilating
697 *Corynebacterium* strain, ST-10. *Appl Environ Microbiol* 63:3783–3788.
- 698 13. Toda H, Itoh N. 2012. Isolation and characterization of styrene metabolism
699 genes from styrene-assimilating soil bacteria *Rhodococcus* sp. ST-5 and ST-10.
700 *J Biosci Bioeng* 113:12–19.
- 701 14. Marconi AM, Beltrametti F, Bestetti G, Solinas F, Ruzzi M, Galli E, Zennaro E.
702 1996. Cloning and characterization of styrene catabolism genes from
703 *Pseudomonas fluorescens* ST. *Appl Environ Microbiol* 62:121–127.
- 704 15. Arenskötter M, Bröker D, Steinbüchel A. 2004. Biology of the metabolically
705 diverse genus *Gordonia*. *Appl Environ Microbiol* 70:3195–3204.
- 706 16. Drzyzga O. 2012. The strengths and weaknesses of *Gordonia*: a review of an
707 emerging genus with increasing biotechnological potential. *Crit Rev Microbiol*
708 38:300–316.

- 709 17. Oelschlägel M, Zimmerling J, Schlömann M, Tischler D. 2014. Styrene oxide
710 isomerase of *Sphingopyxis* sp. Kp5.2. *Microbiology (Reading, Engl.)* 160:2481–
711 2491.
- 712 18. Oelschlägel M, Kaschabek SR, Zimmerling J, Schlömann M, Tischler D. 2015.
713 Co-metabolic formation of substituted phenylacetic acids by styrene-degrading
714 bacteria. *Biotechnol Rep* 6:20–26.
- 715 19. Esuola CO, Babalola OO, Heine T, Schwabe R, Schlömann M, Tischler D. 2016.
716 Identification and characterization of a FAD-dependent putrescine N-hydroxylase
717 (GorA) from *Gordonia rubripertincta* CWB2. *J Mol Catal B: Enzym* 134:378–389.
- 718 20. Altschul SF, Gish W, Miller W, Myers EW, Lipman DJ. 1990. Basic local
719 alignment search tool. *J Mol Biol* 215:403–410.
- 720 21. Johnston A, Crombie AT, El Khawand M, Sims L, Whited GM, McGenity TJ,
721 Colin Murrell J. 2017. Identification and characterisation of isoprene-degrading
722 bacteria in an estuarine environment. *Environ Microbiol*. doi:10.1111/1462-
723 2920.13842.
- 724 22. Crombie AT, Khawand ME, Rhodius VA, Fengler KA, Miller MC, Whited GM,
725 McGenity TJ, Murrell JC. 2015. Regulation of plasmid-encoded isoprene
726 metabolism in *Rhodococcus*, a representative of an important link in the global
727 isoprene cycle. *Environ Microbiol* 17:3314–3329.
- 728 23. Bai Y, Müller DB, Srinivas G, Garrido-Oter R, Potthoff E, Rott M, Dombrowski N,
729 Munch PC, Spaepen S, Remus-Emsermann M, Huttel B, McHardy AC, Vorholt
730 JA, Schulze-Lefert P. 2015. Functional overlap of the *Arabidopsis* leaf and root
731 microbiota. *Nature* 528:364–369.
- 732 24. Tropel D, van der Meer JR. 2004. Bacterial transcriptional regulators for
733 degradation pathways of aromatic compounds. *Microbiol Mol Biol Rev* 68:474-
734 500.
- 735 25. Kotani T, Yamamoto T, Yurimoto H, Sakai Y, Kato N. 2003. Propane
736 monooxygenase and NAD⁺-dependent secondary alcohol dehydrogenase in
737 propane metabolism by *Gordonia* sp. strain TY-5. *J Bacteriol* 185:7120–7128.
- 738 26. Chan Kwo Chion CK, Askew SE, Leak DJ. 2005. Cloning, expression, and site-
739 directed mutagenesis of the propene monooxygenase genes from
740 *Mycobacterium* sp. strain M156. *Appl Environ Microbiol* 71:1909–1914.
- 741 27. Colby J, Stirling DI, Dalton H. 1977. The soluble methane monooxygenase of
742 *Methylococcus capsulatus* (Bath). Its ability to oxygenate n-alkanes, n-alkenes,
743 ethers, and alicyclic, aromatic and heterocyclic compounds. *Biochem J* 165:395–
744 402.
- 745 28. Furuya T, Hirose S, Osanai H, Semba H, Kino K. 2011. Identification of the
746 monooxygenase gene clusters responsible for the regioselective oxidation of
747 phenol to hydroquinone in mycobacteria. *Appl Environ Microbiol* 77:1214–1220.
- 748 29. Furuya T, Hayashi M, Kino K. 2013. Reconstitution of active mycobacterial
749 binuclear iron monooxygenase complex in *Escherichia coli*. *Appl Environ*
750 *Microbiol* 79:6033–6039.
- 751 30. Furuya T, Hayashi M, Semba H, Kino K. 2013. The mycobacterial binuclear iron
752 monooxygenases require a specific chaperonin-like protein for functional
753 expression in a heterologous host. *FEBS J* 280:817–826.

- 754 31. Narancic T, Djokic L, Kenny ST, O'Connor KE, Radulovic V, Nikodinovic-Runic J,
755 Vasiljevic B. 2012. Metabolic versatility of Gram-positive microbial isolates from
756 contaminated river sediments. *J Hazard Mater* 215-216:243–251.
- 757 32. Braun-Lüllemann A, Majcherczyk A, Hüttermann A. 1997. Degradation of styrene
758 by white-rot fungi. *Appl Microbiol Biotechnol* 47:150–155.
- 759 33. Gaszczak A, Bartelmus G, Gren I. 2012. Kinetics of styrene biodegradation by
760 *Pseudomonas* sp. E-93486. *Appl Microbiol Biotechnol* 93:565–573.
- 761 34. Bredholt H, Josefsen K, Vatland A, Bruheim P, Eimhjellen K. 1998.
762 Emulsification of crude oil by an alkane-oxidizing *Rhodococcus* species isolated
763 from seawater. *Can J Microbiol* 44:330–340.
- 764 35. Lang S, Philp JC. 1998. Surface-active lipids in rhodococci. *Antonie Van*
765 *Leeuwenhoek* 74:59–70.
- 766 36. Franzetti A, Bestetti G, Caredda P, La Colla P, Tamburini E. 2008. Surface-
767 active compounds and their role in the access to hydrocarbons in *Gordonia*
768 strains. *FEMS Microbiol Ecol* 63:238–248.
- 769 37. O'Connor K, Buckley CM, Hartmans S, Dobson AD. 1995. Possible regulatory
770 role for nonaromatic carbon sources in styrene degradation by *Pseudomonas*
771 *putida* CA-3. *Appl Environ Microbiol* 61:544–548.
- 772 38. Velasco A, Alonso S, Garcia JL, Perera J, Diaz E. 1998. Genetic and functional
773 analysis of the styrene catabolic cluster of *Pseudomonas* sp. strain Y2. *J*
774 *Bacteriol* 180:1063–1071.
- 775 39. Santos PM, Blatny JM, Di Bartolo I, Valla S, Zennaro E. 2000. Physiological
776 analysis of the expression of the styrene degradation gene cluster in
777 *Pseudomonas fluorescens* ST. *Appl Environ Microbiol* 66:1305–1310.
778 doi:10.1128/AEM.66.4.1305-1310.2000.
- 779 40. O'Leary ND, O'Connor KE, Duetz W, Dobson AD. 2001. Transcriptional
780 regulation of styrene degradation in *Pseudomonas putida* CA-3. *Microbiology*
781 (Reading, Engl.) 147:973–979.
- 782 41. Leoni L, Ascenzi P, Bocedi A, Rampioni G, Castellini L, Zennaro E. 2003.
783 Styrene-catabolism regulation in *Pseudomonas fluorescens* ST: phosphorylation
784 of StyR induces dimerization and cooperative DNA-binding. *Biochem Biophys*
785 *Res Commun* 303:926–931.
- 786 42. Leoni L, Rampioni G, Di Stefano V, Zennaro E. 2005. Dual role of response
787 regulator StyR in styrene catabolism regulation. *Appl Environ Microbiol* 71:5411–
788 5419.
- 789 43. Milani M, Leoni L, Rampioni G, Zennaro E, Ascenzi P, Bolognesi M. 2005. An
790 active-like structure in the unphosphorylated StyR response regulator suggests a
791 phosphorylation-dependent allosteric activation mechanism. *Structure* 13:1289–
792 1297.
- 793 44. del Peso-Santos T, Shingler V, Perera J. 2008. The styrene-responsive
794 StyS/StyR regulation system controls expression of an auxiliary phenylacetyl-
795 coenzyme A ligase. Implications for rapid metabolic coupling of the styrene
796 upper- and lower-degradative pathways. *Mol Microbiol* 69:317–330.
- 797 45. Patrauchan MA, Florizone C, Eapen S, Gomez-Gil L, Sethuraman B, Fukuda M,
798 Davies J, Mohn WW, Eltis LD. 2008. Roles of ring-hydroxylating dioxygenases in

- 799 styrene and benzene catabolism in *Rhodococcus jostii* RHA1. J Bacteriol
800 190:37–47.
- 801 46. Nikodinovic-Runic J, Flanagan M, Hume AR, Cagney G, O'Connor KE. 2009.
802 Analysis of the *Pseudomonas putida* CA-3 proteome during growth on styrene
803 under nitrogen-limiting and non-limiting conditions. Microbiology (Reading, Engl.)
804 155:3348–3361.
- 805 47. Mooney A, O'Leary ND, Dobson ADW. 2006. Cloning and functional
806 characterization of the styE gene, involved in styrene transport in *Pseudomonas*
807 *putida* CA-3. Appl Environ Microbiol 72:1302–1309. doi:10.1128/AEM.72.2.1302-
808 1309.2006.
- 809 48. Riedel A, Heine T, Westphal AH, Conrad C, Rathsack P, van Berkel WJH,
810 Tischler D. 2015. Catalytic and hydrodynamic properties of styrene
811 monooxygenases from *Rhodococcus opacus* 1CP are modulated by cofactor
812 binding. AMB Express 5:112.
- 813 49. Otto K, Hofstetter K, Röthlisberger M, Witholt B, Schmid A. 2004. Biochemical
814 characterization of StyAB from *Pseudomonas* sp. strain VLB120 as a two-
815 component flavin-diffusible monooxygenase. J Bacteriol 186:5292–5302.
- 816 50. Toda H, Imae R, Komio T, Itoh N. 2012. Expression and characterization of
817 styrene monooxygenases of *Rhodococcus* sp. ST-5 and ST-10 for synthesizing
818 enantiopure (S)-epoxides. Appl Microbiol Biotechnol 96:407–418.
- 819 51. Cheng L, Yin S, Chen M, Sun B, Hao S, Wang C. 2016. Enhancing indigo
820 production by over-expression of the styrene monooxygenase in *Pseudomonas*
821 *putida*. Curr Microbiol 73:248–254.
- 822 52. Han JH, Park MS, Bae JW, Lee EY, Yoon YJ, Lee S-G, Park S. 2006. Production
823 of (S)-styrene oxide using styrene oxide isomerase negative mutant of
824 *Pseudomonas putida* SN1. Enzyme Microb Technol 39:1264–1269.
- 825 53. Oelschlägel M, Gröning JAD, Tischler D, Kaschabek SR, Schlömann M. 2012.
826 Styrene oxide isomerase of *Rhodococcus opacus* 1CP, a highly stable and
827 considerably active enzyme. Appl Environ Microbiol 78:4330–4337.
- 828 54. El Khawand M, Crombie AT, Johnston A, Vavline DV, McAuliffe JC, Latone JA,
829 Primak YA, Lee S-K, Whited GM, McGenity TJ, Murrell JC. 2016. Isolation of
830 isoprene degrading bacteria from soils, development of *isoA* gene probes and
831 identification of the active isoprene-degrading soil community using DNA-stable
832 isotope probing. Environ Microbiol 18:2743–2753.
- 833 55. Alvarez LA, Exton DA, Timmis KN, Suggett DJ, McGenity TJ. 2009.
834 Characterization of marine isoprene-degrading communities. Environ Microbiol
835 11:3280–3291.
- 836 56. van Hylckama VJ, Kingma J, van den Wijngaard, A J, Janssen DB. 1998. A
837 glutathione S-transferase with activity towards cis-1,2-dichloroepoxyethane is
838 involved in isoprene utilization by *Rhodococcus* sp. strain AD45. Appl Environ
839 Microbiol 64:2800–2805.
- 840 57. van Hylckama VJ, Kingma J, Kruizinga W, Janssen DB. 1999. Purification of a
841 glutathione S-transferase and a glutathione conjugate-specific dehydrogenase
842 involved in isoprene metabolism in *Rhodococcus* sp. strain AD45. J Bacteriol
843 181:2094–2101.

- 844 58. van Hylckama VJ, Leemhuis H, Spelberg JHL, Janssen DB, Spelberg JH, van
845 Hylckama Vlieg JE. 2000. Characterization of the gene cluster involved in
846 isoprene metabolism in *Rhodococcus* sp. strain AD45. *J Bacteriol* 182:1956–
847 1963.
- 848 59. El Khawand M. 2014. Bacterial degradation of isoprene in the terrestrial
849 environment. Dissertation. University of East Anglia, Norwich.
- 850 60. Smirnova GV, Oktyabrsky ON. 2005. Glutathione in bacteria. *Biochem (Moscow)*
851 70:1199–1211.
- 852 61. Zimmerling J, Tischler D, Grossmann C, Schlömann M, Oelschlägel M. 2017.
853 Characterization of aldehyde dehydrogenases applying an enzyme assay with *in*
854 *situ* formation of phenylacetaldehydes. *Appl Biochem Biotechnol*:1–13.
- 855 62. Fall R, Copley SD. 2000. Bacterial sources and sinks of isoprene, a reactive
856 atmospheric hydrocarbon. *Environ Microbiol* 2:123–130.
- 857 63. Allocati N, Federici L, Masulli M, Di Ilio C. 2009. Glutathione transferases in
858 bacteria. *FEBS J* 276:58–75.
- 859 64. Fahey RC, Brown WC, Adams WB, Worsham MB. 1978. Occurrence of
860 glutathione in bacteria. *J Bacteriol* 133:1126–1129.
- 861 65. Johnson T, Newton GL, Fahey RC, Rawat M. 2009. Unusual production of
862 glutathione in Actinobacteria. *Arch Microbiol* 191:89–93.
- 863 66. Allocati N, Federici L, Masulli M, Di Ilio C. 2012. Distribution of glutathione
864 transferases in Gram-positive bacteria and Archaea. *Biochimie* 94:588–596.
- 865 67. Navarro-Llorens JM, Patrauchan MA, Stewart GR, Davies JE, Eltis LD, Mohn
866 WW. 2005. Phenylacetate catabolism in *Rhodococcus* sp. strain RHA1: a central
867 pathway for degradation of aromatic compounds. *J Bacteriol* 187:4497–4504.
- 868 68. Chen X, Kohl TA, Rückert C, Rodionov DA, Li L-H, Ding J-Y, Kalinowski J, Liu S-
869 J. 2012. Phenylacetic acid catabolism and its transcriptional regulation in
870 *Corynebacterium glutamicum*. *Appl Environ Microbiol* 78:5796–5804.
- 871 69. van Hylckama VJ, Janssen DB. 2001. Formation and detoxification of reactive
872 intermediates in the metabolism of chlorinated ethenes. *J Biotechnol* 85:81–102.
- 873 70. Rui L, Kwon YM, Reardon KF, Wood TK. 2004. Metabolic pathway engineering
874 to enhance aerobic degradation of chlorinated ethenes and to reduce their
875 toxicity by cloning a novel glutathione S-transferase, an evolved toluene o-
876 monooxygenase, and gamma-glutamylcysteine synthetase. *Environ Microbiol*
877 6:491–500.
- 878 71. Dorn E, Hellwig M, Reineke W, Knackmuss H-J. 1974. Isolation and
879 characterization of a 3-chlorobenzoate degrading pseudomonad. *Arch Microbiol*
880 99:61–70.
- 881 72. Cooper DG, Goldenberg BG. 1987. Surface-active agents from two bacillus
882 species. *Appl Environ Microbiol* 53:224–229.
- 883 73. Ames-Gottfred NP, Christie BR, Jordan DC. 1989. Use of the Chrome Azurol S
884 agar plate technique to differentiate strains and field isolates of *Rhizobium*
885 *leguminosarum* biovar *trifolii*. *Appl Environ Microbiol* 55:707–710.
- 886 74. Gordon D, Abajian C, Green P. 1998. Consed: a graphical tool for sequence
887 finishing. *Genome Res* 8:195–202.
- 888 75. Gordon D, Green P. 2013. Consed. A graphical editor for next-generation
889 sequencing. *Bioinformatics* 29:2936–2937.

- 890 76. Seemann T. 2014. Prokka: rapid prokaryotic genome annotation. *Bioinformatics*
891 30:2068–2069.
- 892 77. Krogh A, Larsson B, Heijne G von, Sonnhammer EL. 2001. Predicting
893 transmembrane protein topology with a hidden Markov model: application to
894 complete genomes. *J Mol Biol* 305:567–580.
- 895 78. Bertelli C, Laird MR, Williams KP, Lau BY, Hoad G, Winsor GL, Brinkman FS.
896 2017. IslandViewer 4. Expanded prediction of genomic islands for larger-scale
897 datasets. *Nucleic Acids Res.* doi:10.1093/nar/gkx343.
- 898 79. Langmead B, Salzberg SL. 2012. Fast gapped-read alignment with Bowtie 2. *Nat*
899 *Methods* 9:357–359.
- 900 80. Hilker R, Stadermann KB, Schwengers O, Anisiforov E, Jaenicke S, Weisshaar
901 B, Zimmermann T, Goesmann A. 2016. ReadXplorer 2-detailed read mapping
902 analysis and visualization from one single source. *Bioinformatics* 32:3702–3708.
- 903 81. Shevchenko A, Tomas H, Havlis J, Olsen JV, Mann M. 2006. In-gel digestion for
904 mass spectrometric characterization of proteins and proteomes. *Nat Protoc*
905 1:2856–2860.
- 906 82. Al-Furoukh N, Ianni A, Nolte H, Hölper S, Krüger M, Wanrooij S, Braun T. 2015.
907 ClpX stimulates the mitochondrial unfolded protein response (UPRmt) in
908 mammalian cells. *Biochim Biophys Acta* 1853:2580–2591.
- 909 83. Rappsilber J, Mann M, Ishihama Y. 2007. Protocol for micro-purification,
910 enrichment, pre-fractionation and storage of peptides for proteomics using
911 StageTips. *Nat Protoc* 2:1896–1906.
- 912 84. Thakur SS, Geiger T, Chatterjee B, Bandilla P, Fröhlich F, Cox J, Mann M. 2011.
913 Deep and highly sensitive proteome coverage by LC-MS/MS without
914 prefractionation. *Mol Cell Proteomics* 10:M110.003699.
- 915 85. Cox J, Hein MY, Luber CA, Paron I, Nagaraj N, Mann M. 2014. Accurate
916 proteome-wide label-free quantification by delayed normalization and maximal
917 peptide ratio extraction, termed MaxLFQ. *Mol Cell Proteomics* 13:2513–2526.
- 918 86. Puigbo P, Guzman E, Romeu A, Garcia-Vallve S. 2007. OPTIMIZER: a web
919 server for optimizing the codon usage of DNA sequences. *Nucleic Acids Res*
920 35:W126-W131.
- 921 87. Sambrook J, Russell DW (ed.). 2001. *Molecular cloning. A laboratory manual,*
922 3rd ed. Cold Spring Harbor Laboratory Press, Cold Spring Harbor, NY.
- 923 88. O'Connor KE, Dobson AD, Hartmans S. 1997. Indigo formation by
924 microorganisms expressing styrene monooxygenase activity. *Appl Environ*
925 *Microbiol* 63:4287–4291.
- 926 89. Warhurst AM, Clarke KF, Hill RA, Holt RA, Fewson CA. 1994. Metabolism of
927 styrene by *Rhodococcus rhodochrous* NCIMB 13259. *Appl Environ Microbiol*
928 60:1137–1145.
- 929 90. Tischler D, Eulberg D, Lakner S, Kaschabek SR, van Berkel WJH, Schlömann M.
930 2009. Identification of a novel self-sufficient styrene monooxygenase from
931 *Rhodococcus opacus* 1CP. *J Bacteriol* 191:4996–5009.
- 932 91. Dawson, R. M. C. 1986. *Data for biochemical research*, 3rd ed. Clarendon Press,
933 Oxford.
- 934 92. Bradford MM. 1976. A rapid and sensitive method for the quantitation of
935 microgram quantities of protein utilizing the principle of protein-dye binding. *Anal*
936 *Biochem* 72:248–254.
- 937 93. Alonso S, Bartolomé-Martín D, del Álamo M, Díaz E, García JL, Perera J. 2003.
938 Genetic characterization of the styrene lower catabolic pathway of *Pseudomonas*
939 sp. strain Y2. *Gene* 319:71–83.

- 940 94. El-Said Mohamed M. 2000. Biochemical and molecular characterization of
941 phenylacetate-coenzyme A ligase, an enzyme catalyzing the first step in aerobic
942 metabolism of phenylacetic acid in *Azoarcus evansii*. J Bacteriol 182:286–294.
- 943 95. Kendall SL, Burgess P, Balhana R, Withers M, Bokum A ten, Lott JS, Gao C,
944 Uhia-Castro I, Stoker NG. 2010. Cholesterol utilization in mycobacteria is
945 controlled by two TetR-type transcriptional regulators: kstR and kstR2.
946 Microbiology (Reading, Engl.) 156:1362–1371.
- 947 96. Nagy I, Schoofs G, Compennolle F, Proost P, Vanderleyden J, Mot R de. 1995.
948 Degradation of the thiocarbamate herbicide EPTC (S-ethyl
949 dipropylcarbamoate) and biosafening by *Rhodococcus* sp. strain NI86/21
950 involve an inducible cytochrome P-450 system and aldehyde dehydrogenase. J
951 Bacteriol 177:676–687.
- 952 97. Takeo M, Murakami M, Niihara S, Yamamoto K, Nishimura M, Kato D-i, Negoro
953 S. 2008. Mechanism of 4-nitrophenol oxidation in *Rhodococcus* sp. strain PN1:
954 characterization of the two-component 4-nitrophenol hydroxylase and regulation
955 of its expression. J Bacteriol 190:7367–7374.
- 956 98. Beltrametti F, Marconi AM, Bestetti G, Colombo C, Galli E, Ruzzi M, Zennaro E.
957 1997. Sequencing and functional analysis of styrene catabolism genes from
958 *Pseudomonas fluorescens* ST. Appl Environ Microbiol 63:2232–2239.
- 959 99. Wadlington MC, Ladner JE, Stourman NV, Harp JM, Armstrong RN. 2009.
960 Analysis of the structure and function of YfcG from *Escherichia coli* reveals an
961 efficient and unique disulfide bond reductase. Biochem 48:6559–6561.
- 962 100. Mullins EA, Sullivan KL, Kappock TJ. 2013. Function and X-ray crystal
963 structure of *Escherichia coli* YfdE. PLoS One 8:e67901.
- 964 101. Reverchon S, Nasser W, Robert-Baudouy J. 1994. pecS: a locus controlling
965 pectinase, cellulase and blue pigment production in *Erwinia chrysanthemi*. Mol
966 Microbiol 11:1127–1139.
- 967 102. Harris DR, Ward DE, Feasel JM, Lancaster KM, Murphy RD, Mallet TC, Crane
968 EJ3. 2005. Discovery and characterization of a Coenzyme A disulfide reductase
969 from *Pyrococcus horikoshii*. Implications for this disulfide metabolism of
970 anaerobic hyperthermophiles. FEBS J 272:1189–1200.
- 971 103. Zhang CC, Huguenin S, Friry A. 1995. Analysis of genes encoding the cell
972 division protein FtsZ and a glutathione synthetase homologue in the
973 cyanobacterium *Anabaena* sp. PCC 7120. Res Microbiol 146:445–455.
- 974 104. Harth G, Maslesa-Galic S, Tullius MV, Horwitz MA. 2005. All four
975 *Mycobacterium tuberculosis* glnA genes encode glutamine synthetase activities
976 but only GlnA1 is abundantly expressed and essential for bacterial homeostasis.
977 Mol Microbiol 58:1157–1172.
- 978 105. Gupta RS. 1994. Identification of a GroES (CPN10)-related sequence motif in
979 the GroEL (CPN60) chaperonins. Biochem Mol Biol Int 33:591–595.
- 980 106. Hahn J-S, Oh S-Y, Roe J-H. 2002. Role of OxyR as a peroxide-sensing
981 positive regulator in *Streptomyces coelicolor* A3(2). J Bacteriol 184:5214–5222.
- 982 107. Dhandayuthapani S, Zhang Y, Mudd MH, Deretic V. 1996. Oxidative stress
983 response and its role in sensitivity to isoniazid in mycobacteria: characterization
984 and inducibility of ahpC by peroxides in *Mycobacterium smegmatis* and lack of
985 expression in *M. aurum* and *M. tuberculosis*. J Bacteriol 178:3641–3649.
- 986 108. Ramachandran S, Magnuson TS, Crawford DL. 2000. Isolation and analysis of
987 three peroxide sensor regulatory gene homologs ahpC, ahpX and oxyR in
988 *Streptomyces viridosporus* T7A--a lignocellulose degrading actinomycete. DNA
989 Seq 11:51–60.
- 990

991 **FIGURE LEGENDS**

992 **Fig. 1.** Comparison of the styrene degradation cluster of *Gordonia rubripertincta*
993 CWB2 with homologous clusters as found in the strains *Rhodococcus opacus* PD630
994 (Accession: NZ_CP003949) (22), *Rhodococcus* sp. AD45 (NZ_CM003191) (58),
995 *Nocardioides* sp. Root240 (NZ_LMIT01000013), *Aeromicrobium* sp. Root495
996 (NZ_LMFJ01000002), *Rhodococcus* sp. ST-10 (AB594506) (13), *Rhodococcus*
997 *opacus* 1CP (NZ_CP009112, NZ_CP009111) (48), *Pseudomonas* sp. Y2 (AJ000330)
998 (38, 93) and *Sphingopyxis fribergensis* sp. Kp5.2 (CP009122) (17). Subclusters of
999 strain CWB2 are indicated (S1-S4) and gene products are given in the legend
1000 coloured by their (predicted) function. Relevant homologous genes and clusters are
1001 emphasized by interspaced conjunctions. Clusters of marked strains are reported to
1002 be involved in isoprene (●) or styrene (#) degradation.

1003 **Fig. 2.** Degradation of 4 mM (S)-styrene oxide with crude extract of styrene grown
1004 biomass of *Gordonia rubripertincta* CWB2 and 5 mM reduced glutathione (●). Only
1005 minor consumption was detected when excluding either reduced glutathione (○) or
1006 crude extract (X) from the reaction mix.

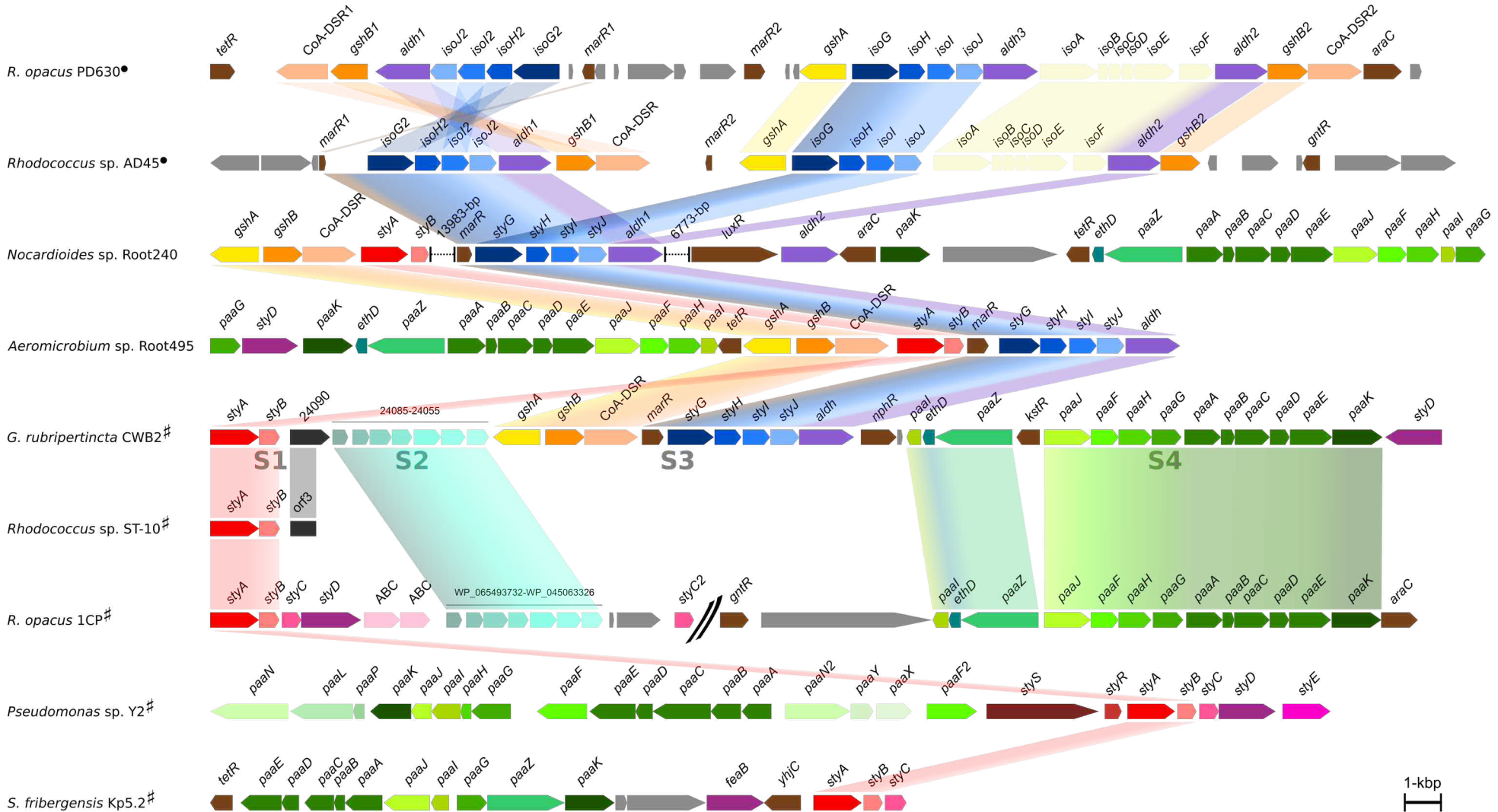
1007 **Fig. 3a.** Proposed novel degradation pathway of styrene in *Gordonia rubripertincta*
1008 CWB2 (see text for details). **3b.** Proposed phenylacetic acid degradation pathway of
1009 *Gordonia rubripertincta* CWB2. The genes of the involved enzymes are present on
1010 the genome (cluster S4) and upregulated on transcriptome and the proteins on
1011 proteome level, respectively (see Table 2). Starting from the product of the upper
1012 degradation pathway, phenylacetic acid, strain CWB2 is able to metabolize styrene to
1013 acetyl-CoA or succinyl-CoA (adapted to 68).

1014 **TABLE LEGENDS**

1015 **Table 1.** Substrate spectra with focus on ones that might be related to styrene
1016 degradation in *G. rubripertincta* CWB2.

1017 **Table 2.** Functional categorization of proteins from *G. rubripertincta* CWB2 that are
1018 supposed to be involved in styrene degradation and regulation on RNA and protein
1019 level. Enzymes and proteins with reported activity or function are underlined. For
1020 further details, see Dataset S1 in supporting material.

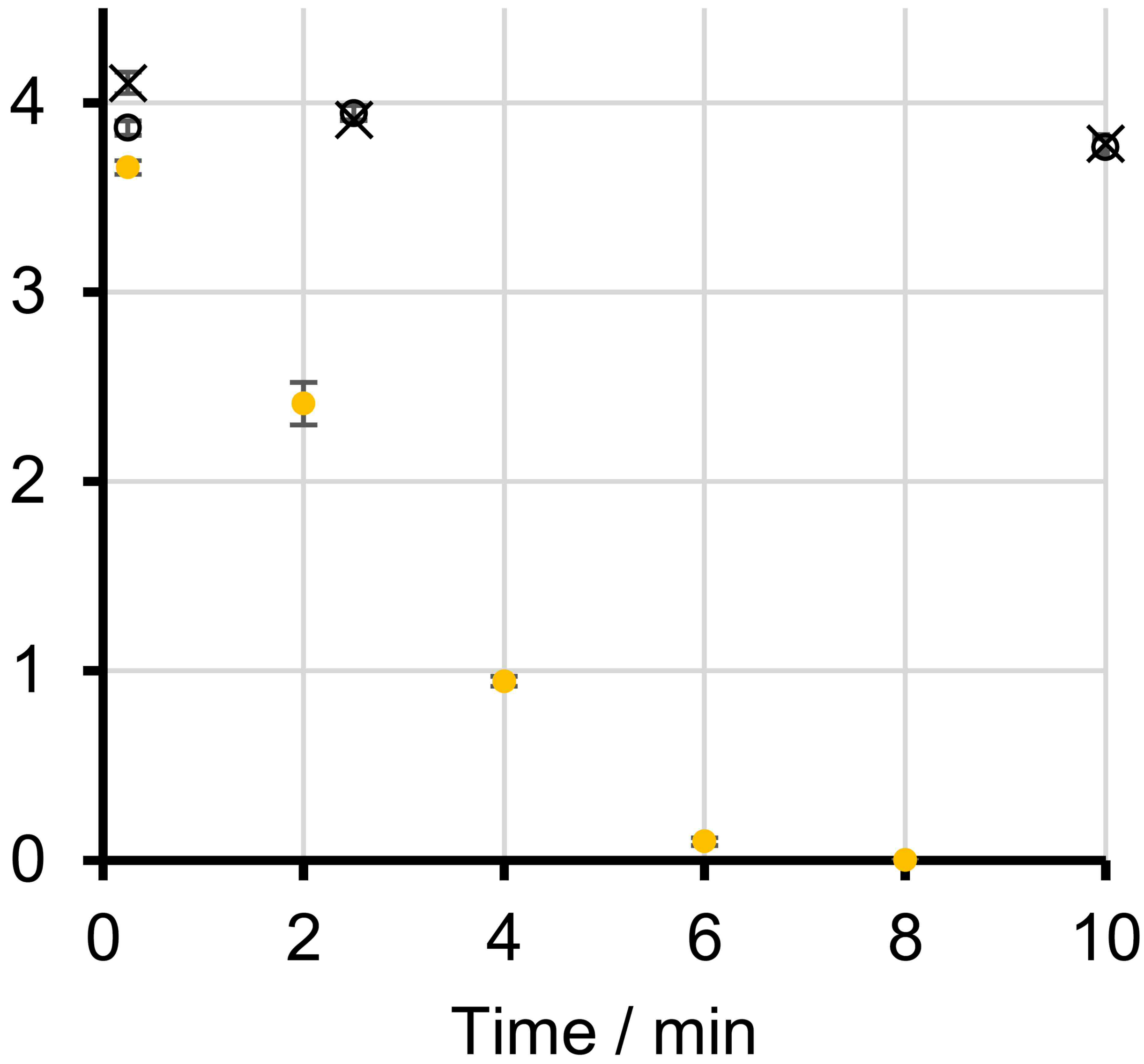
1021 **Table 3.** Plasmids used in this study.



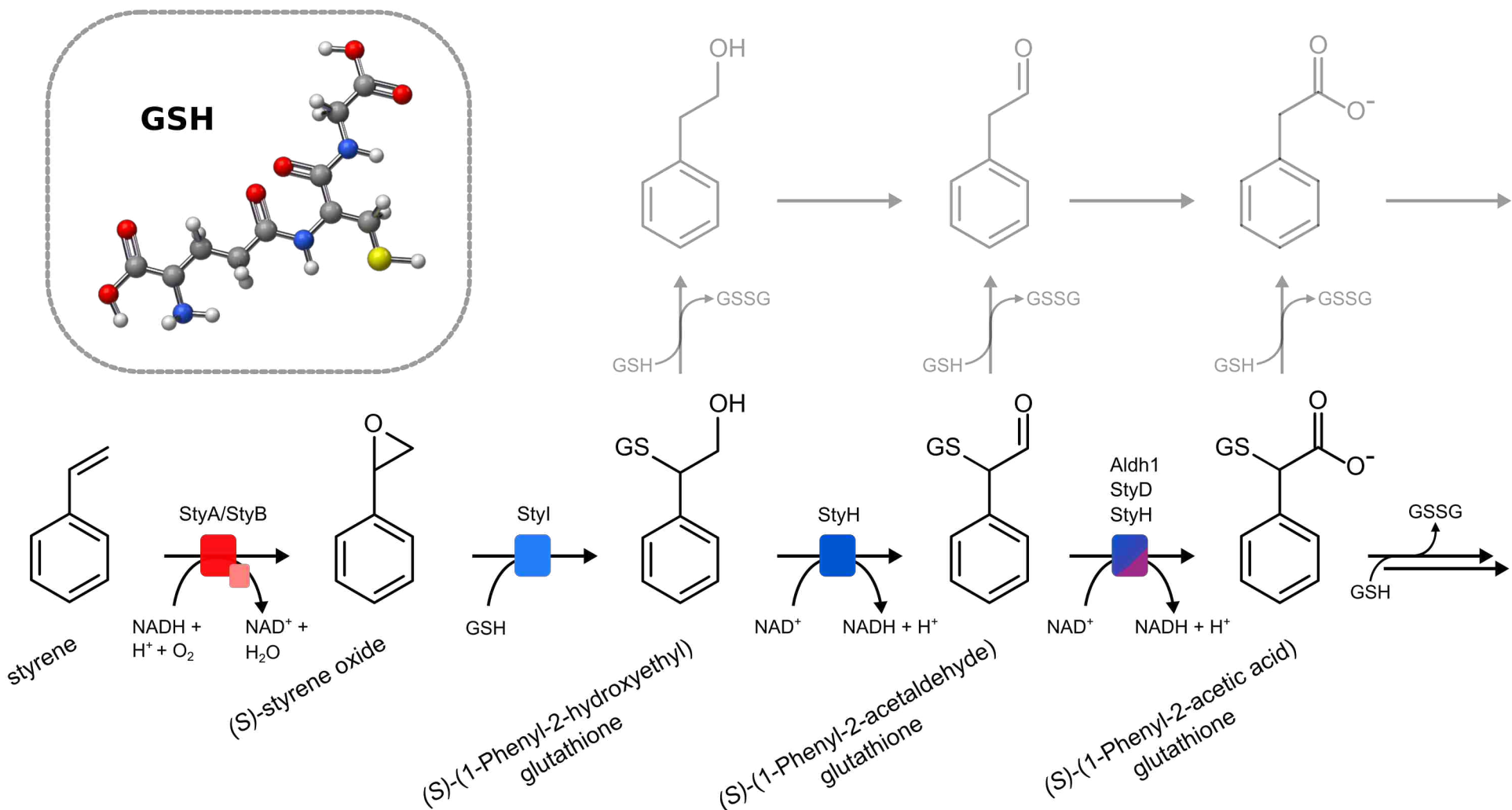
Legend:

Styrene monooxygenase		Glutamate cysteine ligase		1,2-phenylacetyl-CoA epoxidase		Phenylacetate permease		Isoprene monooxygenase	
Styrene oxide isomerase		Glutathione synthetase		2,3-dehydroadipyl-CoA hydratase		Ring opening enzyme		Transcriptional regulator	
Phenylacetaldehyde dehydrogenase		CoA-disulfide reductase		1,2-epoxyphenylacetyl-CoA isomerase		Membrane protein		ABC Transporter	
Sensor kinase		CoA-transferase		3-hydroxyadipyl-CoA dehydrogenase		Transcriptional repressor		Hypothetical protein	
Response regulator		Dehydrogenase		Acyl-CoA thioesterase		Regulator			
ATPase-like transporter		Glutathione-S-transferase		3-oxoadipyl-CoA/3-oxo-5,6-dehydrosuberyl-CoA thiolase		Bifunctional dehydrogenase/hydratase			
Aldehyde dehydrogenase		Glutathione-S-transferase		Phenylacetate-CoA ligase		Ethyl <i>tert</i> -butyl ether protein			

(S)-Styrene oxide / mM



3a. Upper degradation pathway



3b. Lower degradation pathway

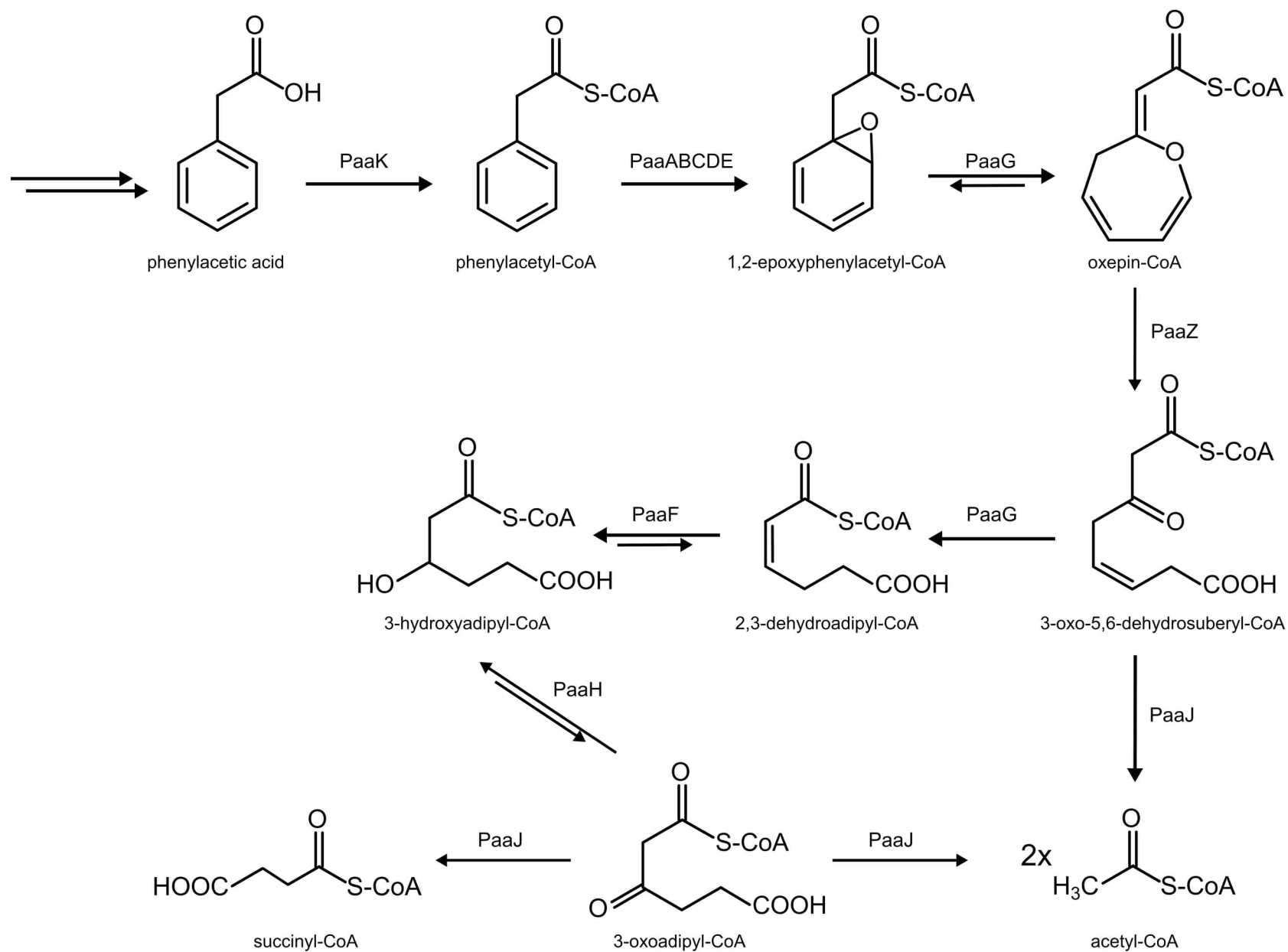


Table 2. Functional categorization of proteins from *G. rubripertincta* CWB2 that are supposed to be involved in styrene degradation and regulation on RNA and protein level. Enzymes and proteins with reported activity or function are underlined. For further details see supporting information.

Transcriptome Proteome						Best hit on the Uniprot Database at amino acid level				
ORF	Gene	A	M	Cyt	Mem	Name*	Function	Accession	% Id	Reference
23925	<u>styD</u>	7.7	8.6	7.1	5.7	<u>styD</u>	Phenylacetaldehyde dehydrogenase	BAL04135	76	(13, 50)
23930	<u>paaK</u>	8.1	6.0	8.1	5.9	<u>paaK</u>	Phenylacetate-coenzyme A ligase	Q9L9C1	68	(94)
23935	<u>paaE</u>	8.0	6.2	11.3	8.2	<u>paaE</u>	1,2-phenylacetyl-CoA epoxidase, subunit E	P76081	43	(8)
23940	<u>paaD</u>	8.1	6.7	NaNf	NaNf	<u>paaD</u>	1,2-phenylacetyl-CoA epoxidase, subunit D	P76080	42	(8)
23945	<u>paaC</u>	8.3	6.7	10.5	7.4	<u>paaC</u>	1,2-phenylacetyl-CoA epoxidase, subunit C	P76079	42	(8)
23950	<u>paaB</u>	8.0	6.8	8.8	9.1	<u>paaB</u>	1,2-phenylacetyl-CoA epoxidase, subunit B	P76078	67	(8)
23955	<u>paaA</u>	8.5	7.1	11.4	9.0	<u>paaA</u>	1,2-phenylacetyl-CoA epoxidase, subunit A	P76077	66	(8)
23960	<u>paaG</u>	7.7	7.4	6.9	6.8	<u>paaG</u>	1,2-epoxyphenylacetyl-CoA isomerase	P77467	37	(8)
23965	<u>paaH</u>	7.6	7.5	7.1	6.2	<u>paaH</u>	3-hydroxyadipyl-CoA dehydrogenase	P76083	36	(8)
23970	<u>paaF</u>	7.1	7.4	7.1	5.8	<u>paaF</u>	2,3-dehydroadipyl-CoA hydratase	P76082	36	(8)
23975	<u>paaJ</u>	6.6	8.2	7.4	6.6	<u>paaJ</u>	3-oxoadipyl-CoA/3-oxo-5,6-dehydrosuberil-CoA thiolase	P0C7L2	55	(8)
23980	<u>tetR</u>	7.3	1.8	2.7	1.8	<u>kstR2</u>	HTH-type transcriptional repressor KstR2	A0R4Z6	25	(95)
23985	<u>paaZ</u>	7.9	6.4	6.8	6.0	<u>paaZ</u>	bifunctional aldehyde dehydrogenase	P77455	51	(8)
23990	<u>ethD</u>	8.4	6.3	5.1	5.7	<u>ethD</u>	Uncharacterized 11.0 kDa protein	P43491	48	(96)
23995	<u>paal</u>	7.3	5.2	NaNf	NaNf	<u>paal</u>	Acyl-coenzyme A thioesterase Paal	P76084	45	(8)
24000	partial	7.3	6.4	NaN	NaN		-	-	-	-
24005	<u>araC</u>	8.0	6.0	4.1	8.4	<u>nphR</u>	Transcriptional activator NphR	B1Q2A8	31	(97)
24010	<u>aldh1</u>	9.6	6.4	6.0	5.5	<u>styD</u>	Phenylacetaldehyde dehydrogenase	O06837	36	(98)
24015	<u>styJ</u>	10.1	6.1	7.7	5.9	<u>yfcG</u>	Disulfide-bond oxidoreductase YfcG	P77526	47	(99)
24020	<u>styl</u>	10.4	6.0	5.0	5.3	<u>isol</u>	Glutathione-S-transferase	WP_045063292	49	(57)
24025	<u>styH</u>	9.5	6.3	5.0	4.8	<u>isoH</u>	1-hydroxy-2-glutathionyl-2-methyl-3-butene DH	WP_045063294	59	(57)
24030	<u>styG</u>	10.0	6.3	6.8	5.5	<u>yfdE</u>	Acetyl-CoA:oxalate CoA-transferase	P76518	33	(100)
24035	<u>marR</u>	10.0	3.5	2.1	2.7	<u>marR</u>	regulatory protein	CAA52427	31	(101)
24040	<u>dsr</u>	9.1	4.7	8.5	4.8	<u>dsr</u>	Coenzyme A disulfide reductase	O58308	34	(102)
24045	<u>gshB</u>	8.9	4.9	5.7	3.8	<u>gshB</u>	Glutathione synthetase	P45480	50	(103)
24050	<u>gshA</u>	9.0	3.4	5.5	-2.2	<u>gshA</u>	Glutamate-cysteine ligase EgtA	P9WPK7	33	(104)

1 **Table 3.** Plasmids used in this study

Plasmid	Relevant characteristic(s)	Source or reference
pET16bP	pET16b with additional multicloning site; allows synthesis of recombinant proteins with an N-terminal His ₁₀ -tag	U. Wehmeyer*
pEX-K2-pSGrA1	<i>GCWB2_24100</i> (1284-bp NdeI/NotI fragment) cloned into pEX-K2 vector	MWG Eurofins
pEX-K2-pSGrA2	<i>GCWB2_21620</i> (1359-bp NdeI/NotI fragment) cloned into pEX-K2 vector	MWG Eurofins
pEX-K2-pSGrD1	<i>GCWB2_23925</i> (1488-bp NdeI/NotI fragment) cloned into pEX-K2 vector	MWG Eurofins
pEX-K2-pSGrD2	<i>GCWB2_24010</i> (1437-bp NdeI/NotI fragment) cloned into pEX-K2 vector	MWG Eurofins
pSGrA1_P01	<i>GCWB2_24100</i> (1284-bp NdeI/NotI fragment) cloned into pET16bP	This study
pSGrA2_P01	<i>GCWB2_21620</i> (1359-bp NdeI/NotI fragment) cloned into pET16bP	This study
pSGrD1_P01	<i>GCWB2_23925</i> (1488-bp NdeI/NotI fragment) cloned into pET16bP	This study
pSGrD2_P01	<i>GCWB2_24010</i> (1437-bp NdeI/NotI fragment) cloned into pET16bP	This study

2 * personal communication

3

4